Contribution to the mechanics of machining

technische hogeschool eindhoven
laboratorium voor mechanische technologie en werkplaatstechniek

rapport nr. 0139

rapport van de sectie: Verspaningsonderzoek

codering: P.7.a.1

titel: Contribution to the Mechanics of Machining

auteur(s): Prof.dr. P.C. Veenstra

trefwoord: Verspanings-leer.

sectieleider: Chr. Bus

hoogleraar: Prof.dr. P.C. Veenstra

samenvatting

Uitgaande van het afschuifmodel van Merchant en aannemend dat er mechanisch evenwicht bestaat tussen gemiddelde waarden van de spanningen in een toestand van vlakke spanning, wordt een hoofdvergelijking afgeleid door te aanvaarden dat de richting van de maximale rek van het materiaal de richting is van de maximale hoofdspanning.
Er wordt aangetoond dat naast de Huber-Hencky voorwaarde voor plastische vloei geen verdere energie voorwaarde noodzakelijk is. De oplossing van de hoofdvergelijking wordt vastgelegd door de heersende spanningstoestand, die kan worden bepaald door de verhouding tussen de waarde van de maximale schuifspanning en de plasticiteitskonstante van het materiaal. Dit geldt ook als vervormingsversteviging optreedt.
De theorie wordt geconfronteerd met experimentele resultaten en een ware spannings-rek kromme, gebaseerd op de theorie, wordt afgeleid.

prognose

datum: 1 juni 1965

aantal blz. 49

geschikt voor publicatie in: C.I.R.P.-Annalen.

Summary

Based on the Merchant shear plane model and assuming global mechanical equilibrium between average values of stress in a state of plane stress, a shear angle relation is derived byidentifying the direction of maximum strain with the direction of maximum principal stress.

It is shown that but the von Mises plasticity condition no particular assumption as to minimum work has to be introduced. The shear angle solution is fixed by the prevalent state of stress, which can be expressed in terms of the ratio between the average value of the maximum shear stress and the plasticity constant of the material machined, which also holds when strain-hardening occurs.

A comparison is made with experimental results and a true strain-stress curve of the work-piece material, as obtained from the present theory as given.

Resumé

Basé sur le modèle de cisaillement de Merchant et supposé qu'une équilibre globale existera entre valeurs moyennes des tensions dans un cas de tension plan, une relation d'angle de cisaillement est déduite par identifier la direction du allongement maximum contre la direction de la tension maximum principale.

Il est demontré que outre la Mises-Huber-Hencky condition de plasticité aucune supposition quelconque sera besoin d'introduire. La résolution de l'angle de cisaillement est complètement fixée par l'état de tension préponderant, étant calé par l'idee de relation de la valeur moyenne de la tension de cisaillement maximum et la constante de plasticité du matériel travaillé. Aussi dans le domaine de tremper ce theorème reste valable.

Enfin un parallèle est tiré entre les résultats expérimentals et une courbe allongement-tension vrai du matériel de la pièce à travailler, obtenue de la théorie présente est montrée.

Zusammenfassung

Gegründet auf dem Merchant'schen Modell des Schervorgangs bei der Zerspanung und mit der Annahme dasz ein Gleichgewicht zwischen mittlere Werte der Spannungen **in einem ebenen Spannungszustand** bestehe, wird mittels Identifizierung der Richtung der Maximaldehnung mit derjenige der maximalen Hauptspannung im System eine Scherwinkelgleichung abgeleitet.

Es wird gezeigt dasz auszer die von Mises-Huber-Hencky Bedingung keine weitere Voraussetzung bezüglich die Minimalarbeit notwendig ist.
Die Lösungen der Schwerwinkelgleichung werden völlig bestimmt von dem herrschenden **Spannungzustand** wie festgelegt durch das Verhältnis zwischen den Wert der maximalen Scherspannung und die Plastizitätskonstante des Materials. Auch im Gebiete der Dehnungsverfestigung bewährt die Theorie seine Gültigkeit.

Die Voraussage der Theorie wird verglichen mit Experimentalergebnisse und eine Dehnungs-Spannungskurve für das bearbeitete Material, wie aus der Theorie hervor geht, wird dargestellt.

Nomenclature and units

σ_1 σ_3	average principal stresses in shear zone	Nm^{-2}
σ_x, σ_y	average normal stresses in shear zone	Nm^{-2}
τ_s	average shear stress in shear plane	Nm^{-2}
τ_{max}	average maximum shear stress in shear zone	Nm^{-2}
φ	shear angle	
β	friction angle	
α	rake angle	
ψ	direction of maximum crystal elongation	with respect
Ω	direction of maximum principal stress	to the shear plane
γ_s	shear strain, $\tan \gamma_s = \tan(\varphi - \alpha) + \cot \varphi$	
k	plasticity constant	Nm^{-2}
σ_ε	true tensile stress = $k\sqrt{3}$	Nm^{-2}
g	$\frac{2\sigma_y}{\sigma_y - \sigma_x}$ stress parameter	
f	$\frac{\tau_{max}}{k}$ ratio factor	
t	feed	m/rev
d	depth of cut	m
r_c	chip thickness ratio	
v	cutting speed	ms^{-1}
e	true strain	
ε	natural strain = $Pn\,(1 + \varepsilon)$	

Contribution to the Mechanics of Machining.

I. Introduction.

During the past decades a number of theories on the mechanics of machining has been published. Some of them investigate the entire state of stress, while otherwise equilibrium between average values of stress is assumed to be present in a geometric model of the cutting process.
All theories are directed towards the formulation of a shear angle relation, which is an accessible equation between measurable quantities predicting an unique steady-state configuration for tool rake and friction angle.
A hypothesis of minimum work is generally introduced in order to secure the uniqueness of the shear angle solution.

It even has been shown (1) that the search for uniqueness might considered being fruitless, as a range of steady-state solutions of the Merchant shear-plane type (2) is to be expected within permissible regions of the characteristic angles describing the geometry and the mechanics of the cutting process.

The present author reconsidered extant theories based on the assumption of global equilibrium between average values of stress.
It will be shown that when identifying the direction of maximum strain with the direction of maximum principal stress a shear angle relation can be formulated.
As to this it is not required to introduce any energy condition.
However when aiming at a shear angle solution an additional assumption has to be made with regard to the prevalent state of stress, which will prove to be equivalent to assuming a value of the maximum shear stress in the system in the case that materials behaving according to the von Mises condition of plasticity are being machined.

As a matter of fact the introduction of the von Mises condition implies accepting an energy condition. The latter however, regards exclusively the deformation of the workpiece material and does not refer to the cutting process as a whole.

A treatment of the problem along these lines will prove to be able to account for the strain-hardening properties of the material.

2. The direction of maximum strain (3), and a shear angle relation.

In the present theory the Merchant shear plane geometric model according to fig. 1 is accepted. The problem will be treated as a case of plane stress. From fig. 1 follows the geometric condition:

$$\sigma_y = \tau_s \tan(\varphi + \beta - \alpha) \qquad \ldots\ldots (1)$$

and hence can be deduced from the Mohr equilibrium condition as represented in fig. 2:

$$\tan(\varphi + \beta - \alpha) = g \cot 2\Omega \quad (4) \qquad \ldots\ldots (2)$$

where the parameter g defines the state of stress. As is clear from the figure this parameter can be expressed in terms of the prevalent stresses:

$$g = \frac{OP}{MP} = \frac{2\sigma_y}{\sigma_y - \sigma_x} \qquad \ldots\ldots (3)$$

Thus g = 1 defines a state of pure shear.

Merchant introduces the angle Ψ as the direction of the maximum value of the crystal elongation in the chip with respect to the shear plane, which can be interpreted as the direction of the maximum value of strain and hence in mechanical respect as the direction of the maximum (tensile) principal stress in the system.

This is expressed by:

$$\Psi = \Omega \qquad \ldots\ldots (4)$$

Now, as shown in fig. 3 an element AF of the workpiece material will be transformed by the cutting process into the state AF'.
Its original position is fixed by an angle p relative to the coordinate system shown in the figure, the position after deformation is defined by the angle q.

The strain resulting from the deformation amounts:

$$e = \frac{AF' - AF}{AF} = \frac{\cos p}{\cos q} - 1 \qquad \ldots\ldots (5)$$

Furthermore follows from fig. 3:

$$\tan q = \tan \gamma_s + \tan p \qquad \ldots\ldots (6)$$

and hence:

$$\cos p = \left[\frac{1}{1+(\tan q - \tan \gamma_s)^2} \right]^{\frac{1}{2}} \qquad \ldots. (7)$$

Combining eqs. 5 and 7:

$$e = \frac{1}{\cos q} \left[\frac{1}{1+(\tan q - \tan \gamma_s)^2} \right]^{\frac{1}{2}} - 1 \qquad \ldots. (8)$$

The direction of the maximum strain in terms of the angle q by now follows from:

$$\frac{de}{dq} = 0$$

which renders:

$$\tan q_{e.max} = \cot \Psi =$$

$$= \frac{1}{2} \tan \gamma_s + \left[\frac{1}{4} \tan^2 \gamma_s + 1 \right]^{\frac{1}{2}} \qquad \ldots. (9)$$

from which easily can be derived:

$$\cot 2\Psi = \frac{1}{2} \tan \gamma_s \qquad \ldots. (10)$$

Using the eqs. 4 and 2 :

$$\tan(\varphi + \beta - \alpha) = \frac{1}{2} g \tan \gamma_s \qquad \ldots. (11)$$

Substitution of the explicite expression for the shear strain in terms of φ and α according to Merchant results in:

$$\tan(\varphi + \beta - \alpha) = \frac{1}{2} g \left[\tan(\varphi - \alpha) + \cot \varphi \right] \qquad \ldots. (12)$$

which is a shear angle relation valid in a state of stress defined by the parameter g.
The value of the maximum strain follows from eqs. 9 and 8:

$$e_{max} = \left[1 + \tan \gamma_s \left\{ \frac{1}{2} \tan \gamma_s + (1 + \frac{1}{4} \tan^2 \gamma_s)^{\frac{1}{2}} \right\} \right]^{\frac{1}{2}} - 1$$

Hence:

$$\varepsilon = \frac{1}{2} \ln \left[1 + \tan \gamma_s \left\{ \frac{1}{2} \tan \gamma_s + (1 + \frac{1}{4} \tan^2 \gamma_s)^{\frac{1}{2}} \right\} \right] \qquad \ldots (13)$$

By now it is possible to derive the shear angle relation eq.11 in a direct way from the Mohr equilibrium diagram fig.2.
According to eqs.4 and 10 the equality holds:

$$\frac{MP}{PQ} = \cot 2\Omega = \tfrac{1}{2} \tan \gamma_s$$

and as: $MP = \tfrac{1}{2} PR$

follows: $\sphericalangle PQR = \gamma_s$

by which a graphical interpretation is obtained of the relation between the shear strain and the characteristic angle $(\varphi + \beta - \alpha)$.
From this follows the shear angle relation:

$$\tan(\varphi + \beta - \alpha) = \frac{OP}{MP} \tfrac{1}{2} \tan \gamma_s$$

and hence:

$$\varepsilon = \frac{OP}{MP}$$

as already has been defined in eq. 3.

Finally is remarked that the shear strain which in origin has been defined merely as a geometric quantity can be expressed in terms of stress, as also can be concluded from fig.2:

$$\tan \gamma_s = \frac{\sigma_x - \sigma_y}{\tau_s}$$

3. The stress parameter g.

In the case that the value of the stress parameter g is known, the shear angle relation eq. 12 allows for a shear angle solution, i.e. the determination of the shear angle in dependance of the friction angle, with the rake angle as a parameter.
As eq. 13 predicts that the strain in the material can be expressed merely in terms of the shear strain, and thus in terms of the shear angle φ, this means that an analytical formulation will be obtained accounting for the interaction between the friction on the rake of the tool - whatsoever the physical background of this particular process might be - and the deformation of the workpiece material in the shear zone. Thus it is important to investigate the physical meaning of the stress parameter g, apart from its definition eq. 3.

The general von Mises plasticity condition reduces to:

$$\sigma_x^2 + \sigma_y^2 - \sigma_x \sigma_y + 3\tau_s^2 = 3k^2 \quad \ldots. (14)$$

in the state of plane stress.
The plasticity constant k is considered being a function of the strain ε, and hence eq. 14 remains valid when strain-hardening occurs.
This means that the plasticity ellipse, when transferred to the coordinate system of principal stresses:

$$\sigma_1^2 + \sigma_3^2 - \sigma_1 \sigma_3 = 3k^2 \quad \ldots. (15)$$

shows semi-axes of variable magnitude in dependance of the state of strain at a given strain rate.

The equilibrium condition according to fig.2 requires:

$$\sigma_x = \sigma_y - 2\tau_s \cot 2\Omega \quad \ldots. (16)$$

The geometric condition as to the stresses has been formulated in eq. 1.

Now the solution of eqs. 1, 14 and 16 refers to a state of stress satisfying simultaneously the geometric condition prescribed by the shear plane model, the condition of global equilibrium and finally the condition of plasticity at the given state of strain and strain rate.

The solution is:

$$\tau_{\varepsilon} = \frac{\kappa\sqrt{3}}{\left[\tan^2(\varphi+\beta-\alpha) - 2\tan(\varphi+\beta-\alpha)\cot 2\Omega + 4\cot^2 2\Omega + 3\right]^{\frac{1}{2}}}$$

$$\sigma_y = \frac{k\sqrt{3}\,\tan(\varphi+\beta-\alpha)}{\left[\tan^2(\varphi+\beta-\alpha) - 2\tan(\varphi+\beta-\alpha)\cot 2\Omega + 4\cot^2 2\Omega + 3\right]^{\frac{1}{2}}} \qquad \ldots(17)$$

while σ_x can be solved from eq.14.

The counterpart of eq.16 also goes from fig. 2:

$$\tau_{\varepsilon} = -\tau_{max}\sin 2\Omega \qquad \ldots(18)$$

and:

$$2\tau_{max} = \sigma_1 - \sigma_3$$

Now two different extreme situations of stress may occur:

1) a state of linear stress:

$$\sigma_1 \neq 0 \qquad \text{or} \qquad \sigma_1 = 0$$
$$\sigma_3 = 0 \qquad\qquad\quad \sigma_3 \neq 0$$

In this case follows from eqs. 15 and 18 :

$$\tau_{max} = \tfrac{1}{2}k\sqrt{3}$$

2) a state of pure shear :

$$\sigma_3 = -\sigma_1$$

where follows from the same equations :

$$\tau_{max} = k$$

In general thus can be put:

$$\tau_{max} = f.k$$

and :

$$\tau_{\varepsilon} = -f\kappa\sin 2\Omega \qquad \ldots(19)$$

where :

$$\tfrac{1}{2}\sqrt{3} < f < 1$$

From this it is clear that any a priori assumption with regard to the value of the maximum shear stress in terms of the plasticity constant defines a state of stress.

In particular the condition $\tau_{max} = k$, which is quite common in extant theories, defines a state of pure shear.

Substitution of eq. 19 into eq. 17 and using eqs. 4 and 10 again leads to a shear angle relation:

$$\tan(\varphi + \beta - \alpha) = \left[1 \pm \left\{3\left(1 + \frac{4}{\tan^2\gamma_s}\right)\left(\frac{1}{f^2} - 1\right)\right\}^{\frac{1}{2}}\right]^{\frac{1}{2}} \tan\gamma_s \quad \ldots(20)$$

Comparison with eq. 11 shows that holds:

$$g = 1 \pm \left[3\left(1 + \frac{4}{\tan^2\gamma_s}\right)\left(\frac{1}{f^2} - 1\right)\right]^{\frac{1}{2}} \quad \ldots(21)$$

from which it is obvious that the state of stress defined in terms of the parameter g at a given state of strain has its physical origin in the ratio f between the average value of the maximum shear stress and the plasticity constant of the material.

The positive sign in eq. 21 implies:

$$|\sigma_y| > \sigma_x$$

the negative sign means:

$$|\sigma_y| < \sigma_x$$

The condition $f = 1$ is compatible with $g = 1$, and defines a state of pure shear, as is shown before.

4. Shear angle solutions.

1. The case of pure shear.

From the foregoing it will be clear that the shear angle relation eq. 20 or 12 reduces to :

$$\tan(\varphi + \beta - \alpha) = \tfrac{1}{2}\left[\tan(\varphi - \alpha) + \cot\varphi\right] \qquad \ldots(22)$$

from which φ can be solved as a function of β , for given values of the rake angle α.

The solution has been plotted in fig. 4, where in the usual way of representation the shear angle φ appears as a function of the angle $\beta - \alpha$.

A remarkable fact is that in the present theory the rake angle operates as a parameter which definitely influences the solution obtained.

This is shown for the values $\alpha = \pm 30^{\circ}$ and $\alpha = 0^{\circ}$.

As a comparison also the Merchant and Lee and Shaffer (5) solutions have been plotted.

The present theory proves to arrive at values intermediate between those predicted by the theories mentioned, as it should do whenever it would have a chance to cover reality. It is observed that in the interval $0 < \varphi < \frac{1}{2}\pi$, the theory apparently does not allow for unique solutions.

As to deal with this it is sufficient to remark that the shear strain passes through a minimum value as a function of the shear angle φ :

$$\frac{d \tan \gamma_s}{d\varphi} = \frac{1}{\cos^2(\varphi - \alpha)} - \frac{1}{\sin^2\varphi} = 0$$

Hence the minimum value of the shear strain is reached at:

$$\varphi = \tfrac{1}{4}\pi + \tfrac{1}{2}\alpha \qquad \ldots(23)$$

where the friction angle β has the value zero as can be checked by substitution of eq.23 into eq. 22.

In this state the cutting process dissipates energy only by deformation of the workpiece material in absence of friction on the rake of the tool.
It seems obvious that this never can be a physical reality and thus the uniqueness of the solution of eq. 22 is secured by:

$$\beta \geqslant 0$$

$$\varphi < \tfrac{1}{4}\pi + \tfrac{1}{2}\alpha \qquad \ldots(24)$$

In the figure 4 the region of physical significance is restricted to :

$\varphi = 30^\circ$ for $\alpha = -30^\circ$, to $\varphi = 45^\circ$ for $\alpha = 0^\circ$ and to

$\varphi = 60^\circ$ for $\alpha = +30^\circ$.

The solutions again prove to be unique.

2. The case of a general state of stress.

As discussed before the state of general stress prevails when:

$$f = \frac{\tau_{max}}{k} < 1$$

The system is governed by the shear angle relation eq.20, from which after expressing the shear strain in terms of shear angle and rake angle, shear angle solutions can be obtained with both f and α as parameters.

As is shown in fig. 5 the ratio f has a very strong influence on the course of the shear angle solution, and so it does in particular in the region close to $f = 1$.

When reading fig. 5 it should be kept in mind that every value of the parameter f gives to two different shear angle solutions, corresponding to the choice of the sign in the eqs. 20 and 21, and hence dependent on the modulus of the ratio between the principal stresses, which can be expressed in terms of $g \gtrless 1$, as shown before.

When is accepted that the average value of the maximum shear stress as a resultant of a hypothetic stress distribution might differ up to about 2% from the plasticity constant of the material machined, quite a number of the observations published in current literature is covered by the present theory.
It even might be that the extreme sensitiviness of the shear angle solution with respect to the state of stress suggests a lack of unique solutions of the problem.

A more complete picture gives fig. 6 where the effect of both of the two parameters is shown simultaneously under the condition $g > 1$, as appears to be usual in a majority of the practical cases investigated.
It is observed that the influence of the rake angle decreases rapidly as the value of f decreases, i.e. when the average behaviour of the system moves out of the state of pure shear.

In conclusion is shown the figure 7 where experimental data as used by Oxley (6) as an example are compared with the present theory.

5. Experimental results.

A major difficulty in verifying shear-angle solutions arises from measuring the shear-angle φ in an accuracy comparable with which can be obtained when measuring the friction angle β by means of dynamometry. As a rule cutting forces will be recorded during a considerable length of time and hence an average value of the friction angle can be determined with fair precision.

On the contrary determination of the shear-angle depends on measuring the chip-ratio from samples of the chip.
A vast number of samples should be taken in order to arrive at an accuracy comparable with the one obtained by dynamometry.

Now, in a program of investigation of cutting temperatures, an extensive study has been made of the behaviour of the chip contact length in relation to the cutting conditions (7).

When machining obliquely an annealed steel C 45 with a carbide tool of the grade S 2 (ISO - P 20)
a definite relation between feed, speed and chip ratio proves to exist:

$$r_c = \frac{0{,}615\ t}{0{,}205.10^{-3} + 0{,}850\ t - 0{,}029.10^{-3} v} \qquad \ldots.(25)$$

in the speed range $1 < v < 5$ ms^{-1}, in the feed range

$0{,}2.10^{-3} < t < 1{,}0.10^{-3}$ m/rev., and at the depth of

cut of $d = 3.10^{-3}$ m.

As eq.25 has been obtained from the study of the average behaviour of the chip contact length as recorded in a natural way in the wear pattern on the rake of the tool, the accuracy in determining the shear-angle from it proves to be about the same as in determining the friction-angle from recordings obtained with a sensitive strain-gage dynamometer (8).

Statistical evaluation shows a relative error of 2% in the shear-angle and a relative error of 2,5% in the angle $\beta - \alpha$.

The experimental results have been plotted in fig. 8, where both values of the shear-angle obtained by use of eq. 25 and those obtained by direct measurement of the chip ratio have been used. The presence of a systematic error is evident.

The agreement with the present shear-angle relation eq. 22 is pretty good, from which it might be concluded that the material is machined in an average state of pure shear, and probably behaves according to the von Mises condition of plasticity.

A second series of experiments has been performed with a negative value of the rake-angle. The results are shown in fig. 9 from which the conclusion might be the same.

In conclusion it is remarked that eq. 17 when used in connection with dynamometric experiments allows for investigation into the plastic behaviour of the workpiece material under machining conditions when assuming validity of the von Mises condition.

When using: $\cot 2\Omega = \frac{1}{2} \tan \gamma_s$,

as has been derived earlier, the eq. 17 can be written like:

$$\sigma_\varepsilon = k\sqrt{3} = \tau_s \left[\tan^2(\varphi + \beta - \alpha) - \tan(\varphi + \beta - \alpha)\tan\gamma_s + \tan^2\gamma_s + 3 \right]^{\frac{1}{2}} \quad \ldots (26)$$

by which the true stress σ_ε is expressed in dynamometric quantities and hence can be calculated from numerical experimental values. The amount of computing work is considerably reduced when is known that the material is machined in a state of pure shear, as in this case eq. 17 reduces to $\tau_s = k \sin 2\Omega$.

As derived in eq. 13 the true strain can be calculated from the prevalent value of the shear strain and thus a stress-strain relation in the region of machining conditions can be plotted.

This is shown in fig. 10 as based on the measurements of fig. 8 when machining an annealed steel C 45. The mechanical properties of the material are illustrated in fig. 11, which represents the true stress-strain relation as obtained from a step by step interrupted tensile test.

The yield point of the material is reached at a true stress of $3.42 \cdot 10^8$ Nm^{-2} (34.2 kgf/mm^2), and fraction occurs at a value of the stress close to 10^9 Nm^{-2} (100 kgf/mm^2).
In the region between, the stress-strain curve behaves almost perfectly in accordance with the power function:

$$\sigma_\varepsilon = 1.18 \cdot 10^9 \, \varepsilon^{0,22}$$

From fig. 10 it may be concluded that in the region of high strain and strain rate, as typical for conditions of machining, approximately holds:

$$\sigma_\varepsilon = 1.56 \cdot 10^9 \, \varepsilon^{1.32}$$

A simultaneous representation of both of the two relations is given in fig. 12.

This preliminary investigation into the plastic behaviour of the material under conditions of machining does not conclude to a significant influence of the cutting speed and hence of the strain rate on the strain hardening. By far the most important factor in strain hardening, refering to the particular material studied, appears to be the value of the strain.

So far, however, no experiments have been performed in the region of strain which links the ultimate values of the quasi-static tensile test with the minimum values achievable in machining, in order to investigate wether some continuous transition from the one region to the other might exist.

References

1. Hill, R. J. Mech.Phys. Solids 3, (1954) 47
2. Merchant, M.E. J. Appl.Phys. 11, (1940) 3 230
   J. Appl.Phys. 16, (1945) 5 267
   J. Appl.Phys. 16, (1945) 6 318
3. Zweekhorst, E.T.W. Metaalbewerking 29, (1964)22 471
4. Colding, B.N. Thesis, Stockholm 1959, p. 39
5. Lee, F.H. and Shaffer, B.W. J. Appl.Mech. 73, (1951) 405
6. * Oxley, P.L.B. Int.J.Mach.Tool Des.Res. 2 (1962) 219
   Prod.Eng. 43 (1964) 609
   Oxley, P.L.B. and Hatton, A.P. Int.J.Mech.Sci. 5 (1963) 41
7. Hulst, A.P.A.J. Lab.research report WT 129, WT 135 Eindhoven (1965)
8. Ten Horn, B.L. Metaalbewerking 24 (1958) 3,39
   and Schürmann, R.A. Metaalbewerking 24 (1958) 5,85

Fig. 1.

The Merchant shear plane model and the geometric stress condition:

$$\sigma_y = \tau_s \tan(\varphi + \beta - \alpha)$$

TECHNISCHE HOGESCHOOL EINDHOVEN

LABORATORIUM VOOR MECHANISCHE TECHNOLOGIE
EN WERKPLAATSTECHNIEK

fig.1.

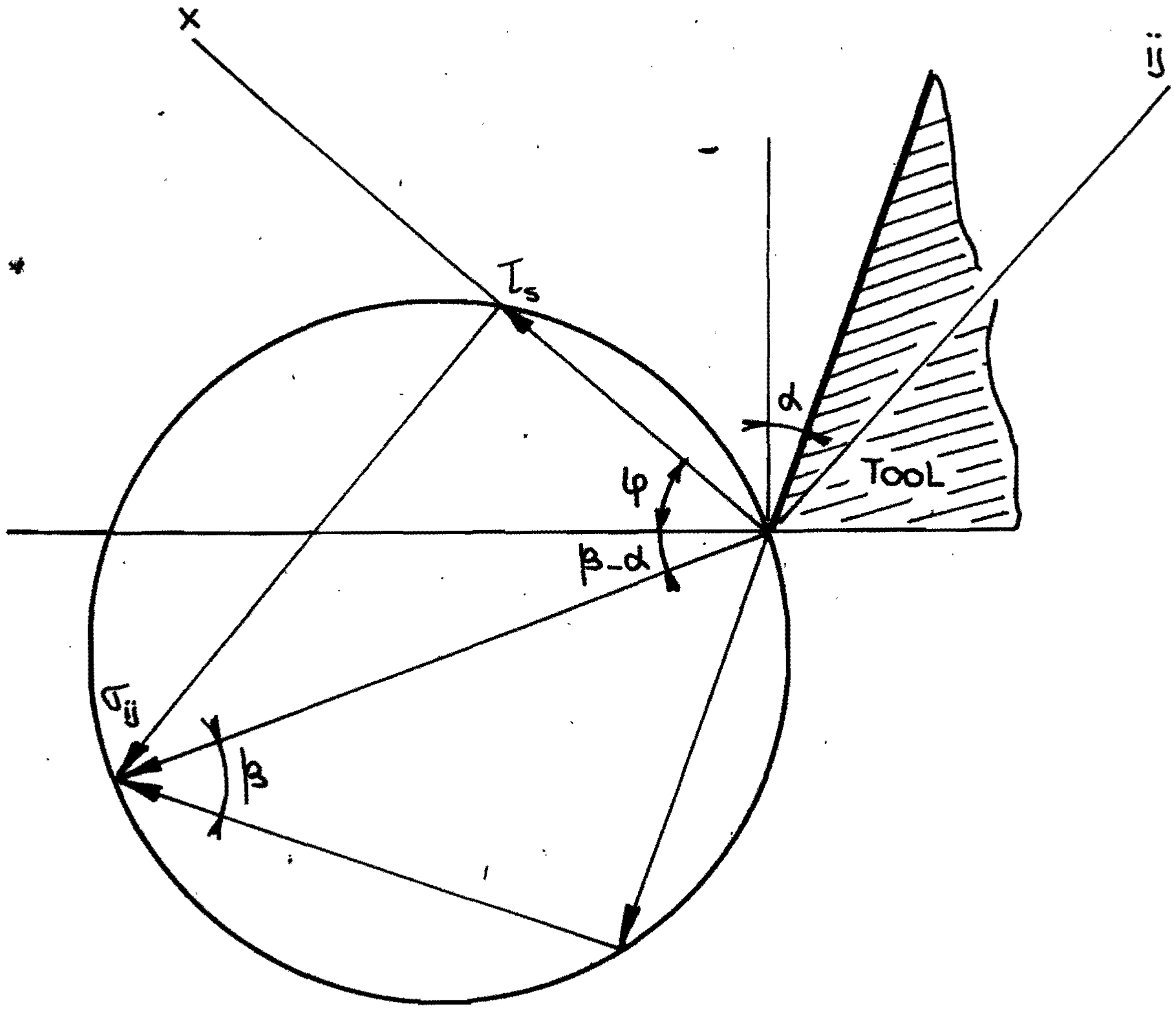

Fig. 2

The Mohr equilibrium condition and the stress parameter

$$g = \frac{OP}{MP} = \frac{2\sigma_y}{\sigma_y - \sigma_x} \quad ,$$ from which is derived:

$$\tan(\varphi + \beta - \alpha) = g \cot 2\Omega$$

If the direction Ω of the maximum principal stress is identified with the direction of maximum strain, it can be shown that holds:

$$\cot 2\Omega = \tfrac{1}{2} \tan \gamma_s$$

from which follows:

$$\sphericalangle\, PQR = \gamma_s$$

and hence the shear angle equation:

$$\tan(\varphi + \beta - \alpha) = \tfrac{1}{2}\, g \tan \gamma_s = \tfrac{1}{2}\, g \left[\tan(\varphi - \alpha) + \cot \varphi \right] .$$

TECHNISCHE HOGESCHOOL EINDHOVEN

LABORATORIUM VOOR MECHANISCHE TECHNOLOGIE EN WERKPLAATSTECHNIEK

fig. 2

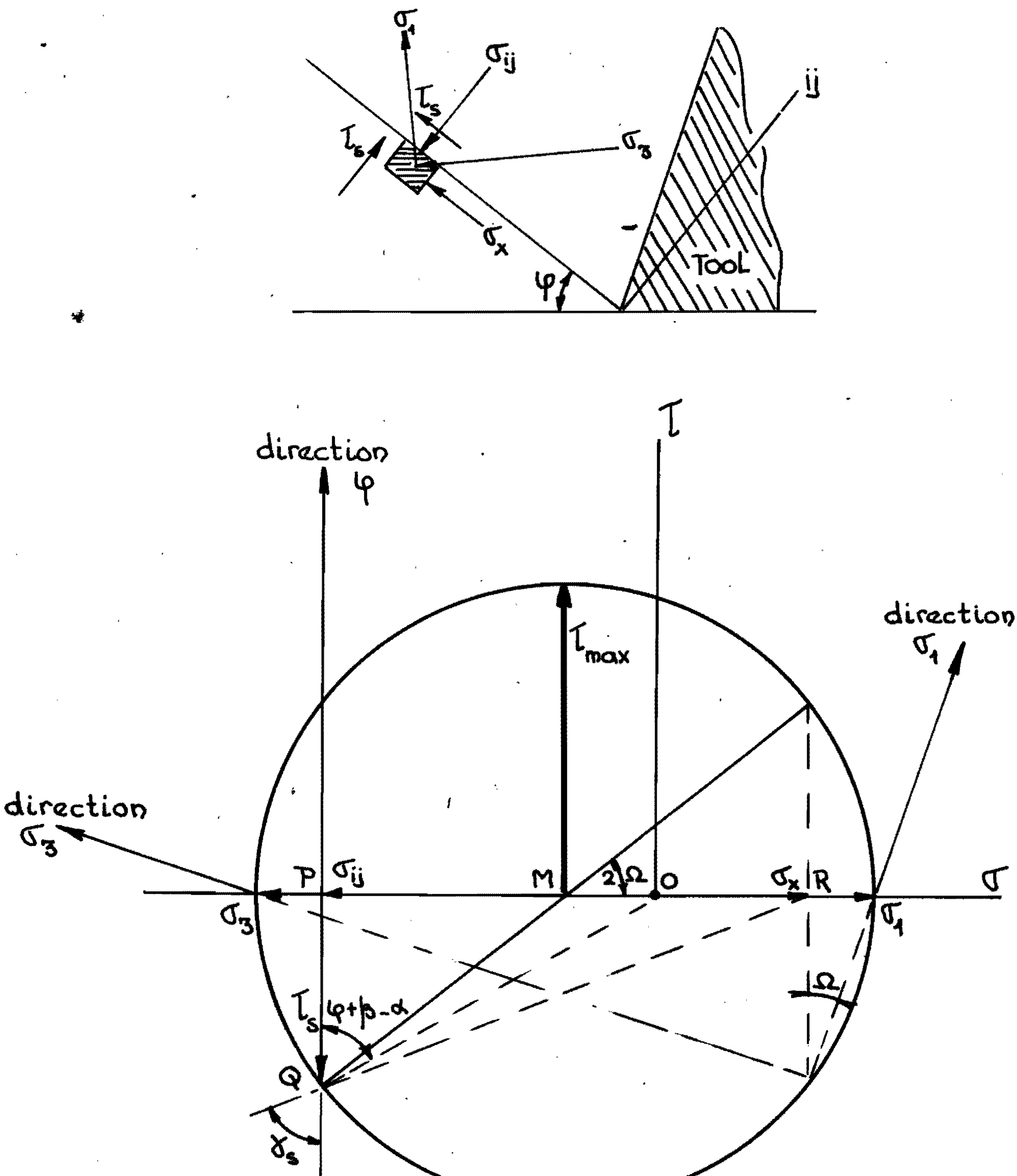

Fig. 3

Determination of the direction $q = \frac{\pi}{2} - \psi = \frac{\pi}{2} - \Omega$ of maximum strain.

An element of material AF is deformed by the cutting proces into the state AF' and is thus strained to the amount

$$\varepsilon = \frac{AF'}{AF} - 1 = \frac{\cos p}{\cos q} - 1$$

From the condition $\frac{d\varepsilon}{dq} = 0$, can be derived the direction of maximum strain:

$$\cot 2\Omega = \tfrac{1}{2} \tan \gamma_s = \cot 2\psi$$

TECHNISCHE HOGESCHOOL EINDHOVEN

LABORATORIUM VOOR MECHANISCHE TECHNOLOGIE
EN WERKPLAATSTECHNIEK

fig. 3

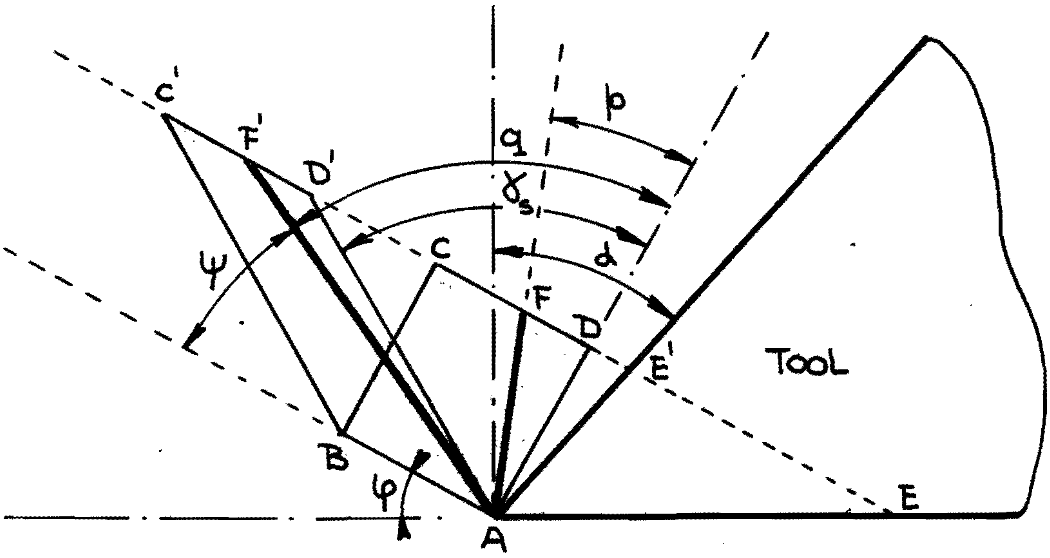

Fig. 4

The shear angle solution eq. 20 in the state of stress of pure shear, as defined by the condition $\sigma_3 = -\sigma_1$ and hence by $\tau_{max} = k$ or $f = g = 1$

Shown is the effect of the rake angle as a parameter.

A comparison is made with both the Merchant and the Lee and Schaffer solutions.

TECHNISCHE HOGESCHOOL EINDHOVEN

LABORATORIUM VOOR MECHANISCHE TECHNOLOGIE EN WERKPLAATSTECHNIEK

fig. 4

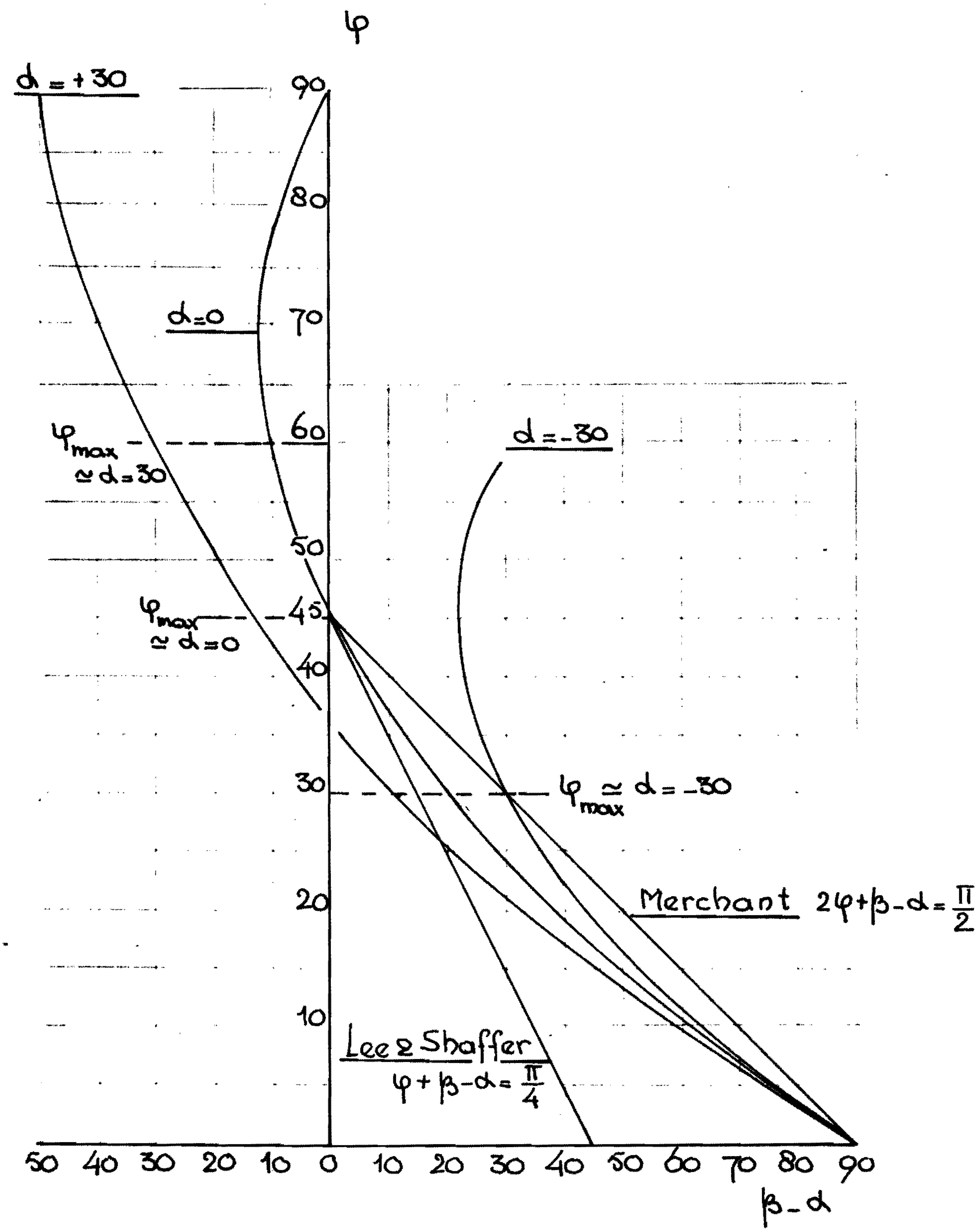

Fig. 5

The shear angle relation eq. 20 for the value of the rake angle $\alpha = 0$ and different values of the ratio

$$f = \frac{\tau_{max}}{k} .$$

Shown is the sensitiveness of the solution with respect to minor changes in f in the region close to f = 1.
Both the possible solutions have been plotted according to the value f = 0,99, corresponding with the two possible different states of average stress.

TECHNISCHE HOGESCHOOL EINDHOVEN

LABORATORIUM VOOR MECHANISCHE TECHNOLOGIE EN WERKPLAATSTECHNIEK

fig. 5

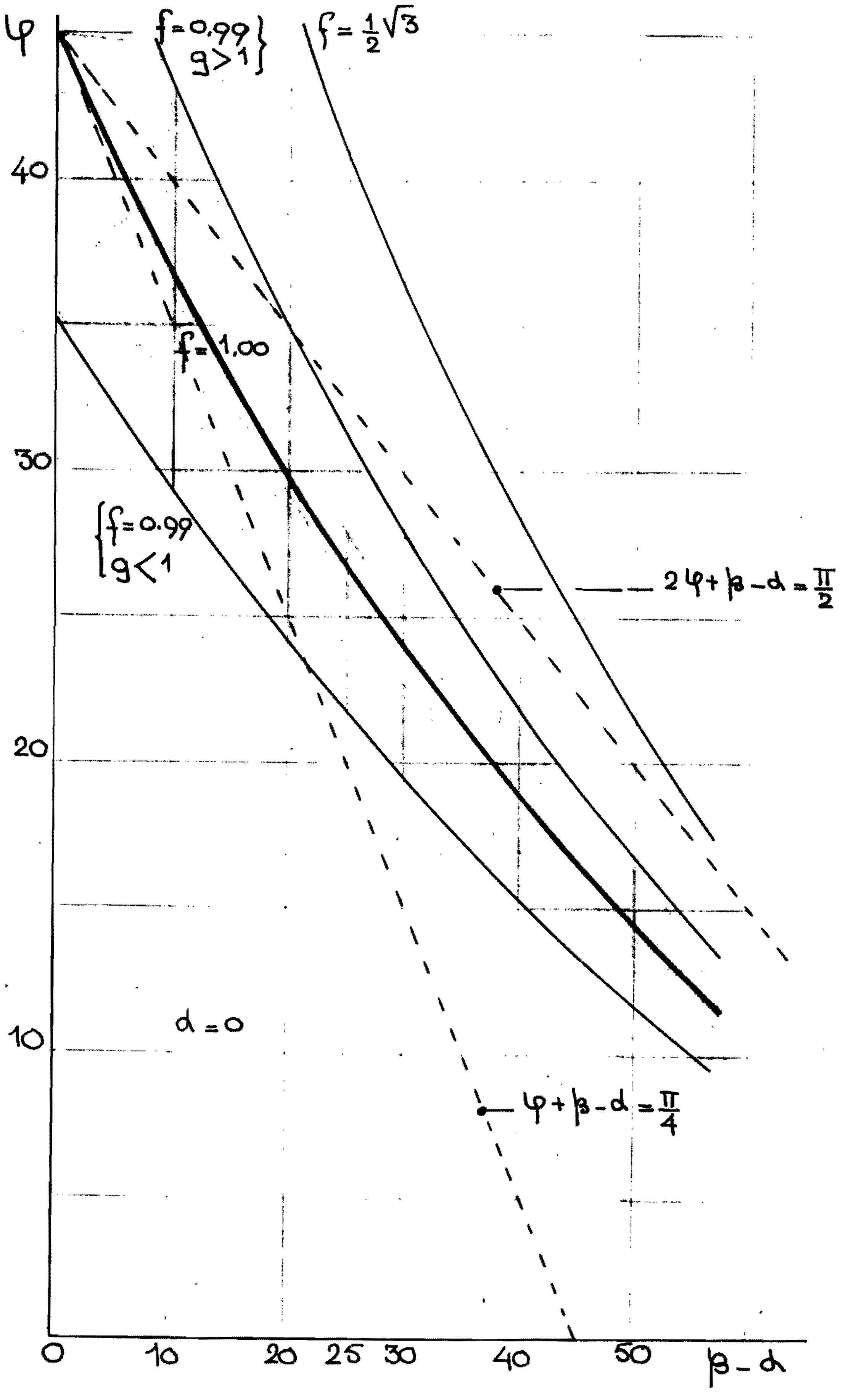

Fig. 6

The shear angle relation eq.20 for different values of both the rake angle α and the ratio f.

Only the solutions corresponding with the positive sign in the eqs. 20 and 21 have been plotted, as will refer to the majority of the practical cases.
To be observed is the decreasing importance of the rake angle as the ratio f decreases due to the moving of the system out of a state of pure shear.

TECHNISCHE HOGESCHOOL EINDHOVEN

LABORATORIUM VOOR MECHANISCHE TECHNOLOGIE
EN WERKPLAATSTECHNIEK

fig. 6

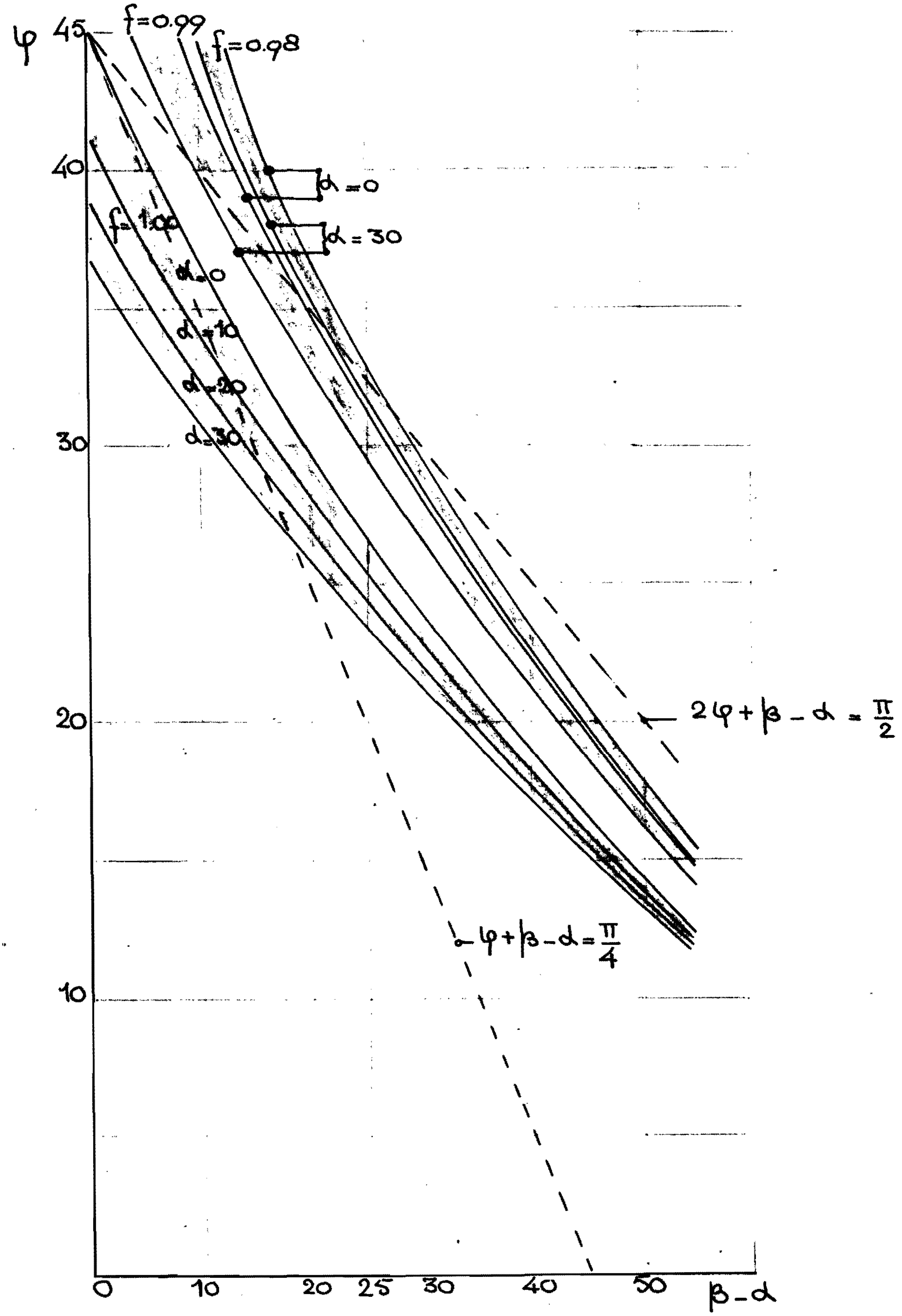

Fig. 7

Comparison of a number of shear angle values as used by Oxley (6) with the predictions of the present theory according to eq. 20.

TECHNISCHE HOGESCHOOL EINDHOVEN

LABORATORIUM VOOR MECHANISCHE TECHNOLOGIE
EN WERKPLAATSTECHNIEK

fig. 7

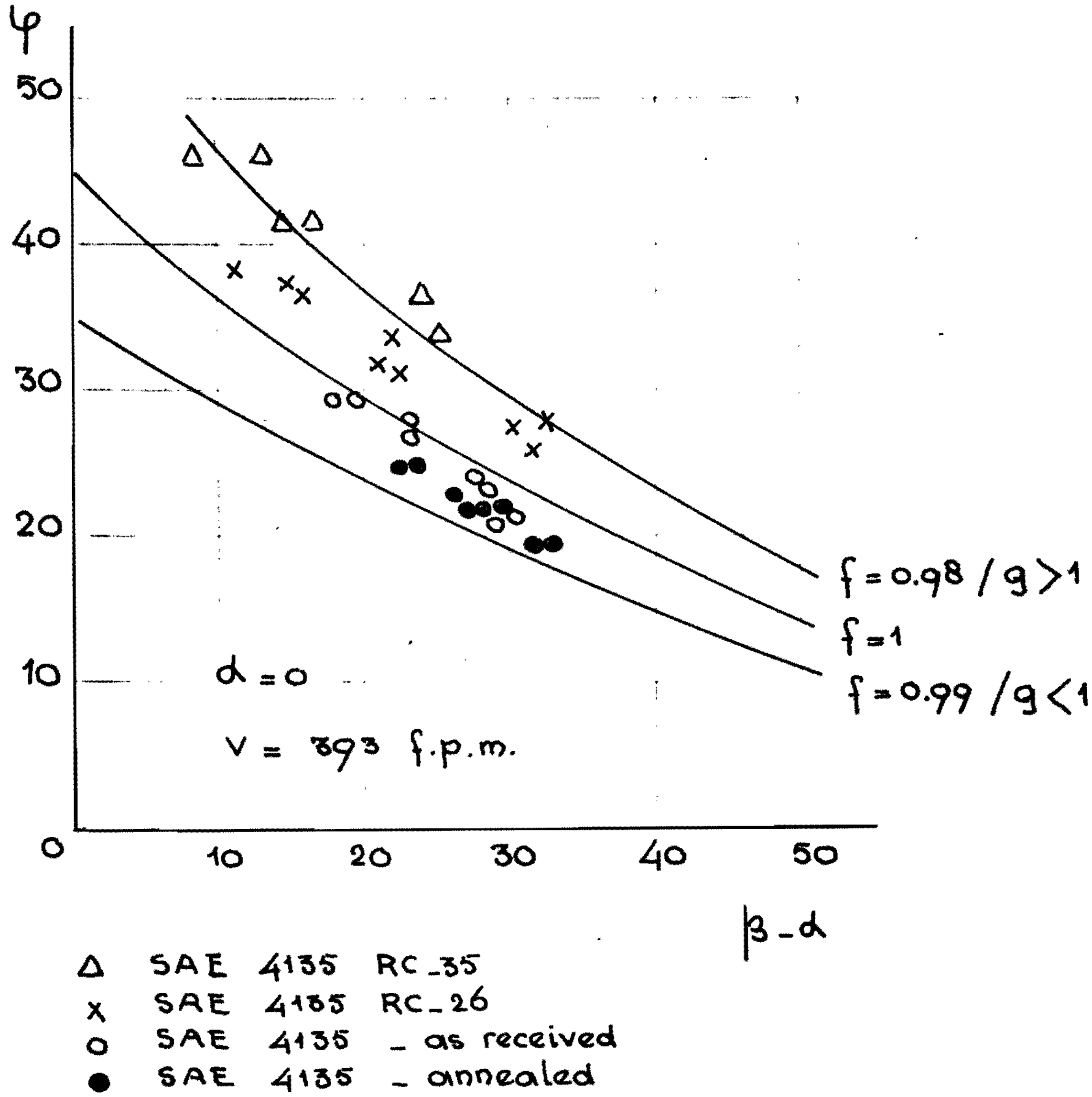

Fig. 8 and fig. 9

Comparison of experimental results with the predictions of the present theory, eq. 22 when machining an annealed steel C 45.

Speed range 1 ÷ 5 ms^{-1}, feed range 0,2 ÷ 1,0 mm/rev, depth of cut 3 mm.

● = determined indirectly from chip ratio relation eq. 25

x = measured directly from chip ratio by sampling.

TECHNISCHE HOGESCHOOL EINDHOVEN

LABORATORIUM VOOR MECHANISCHE TECHNOLOGIE
EN WERKPLAATSTECHNIEK

fig.8

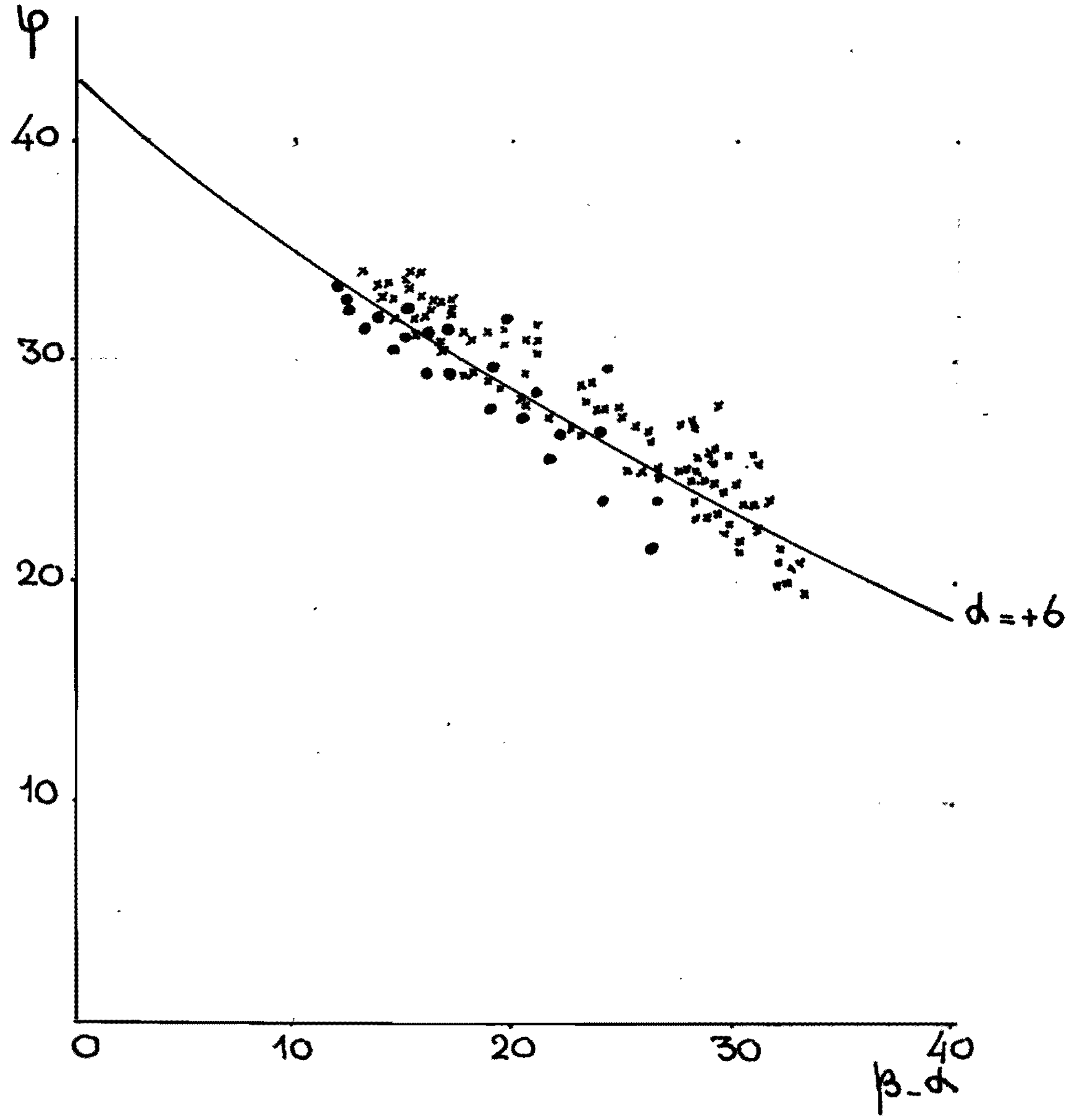

TECHNISCHE HOGESCHOOL EINDHOVEN

LABORATORIUM VOOR MECHANISCHE TECHNOLOGIE EN WERKPLAATSTECHNIEK

fig. 9

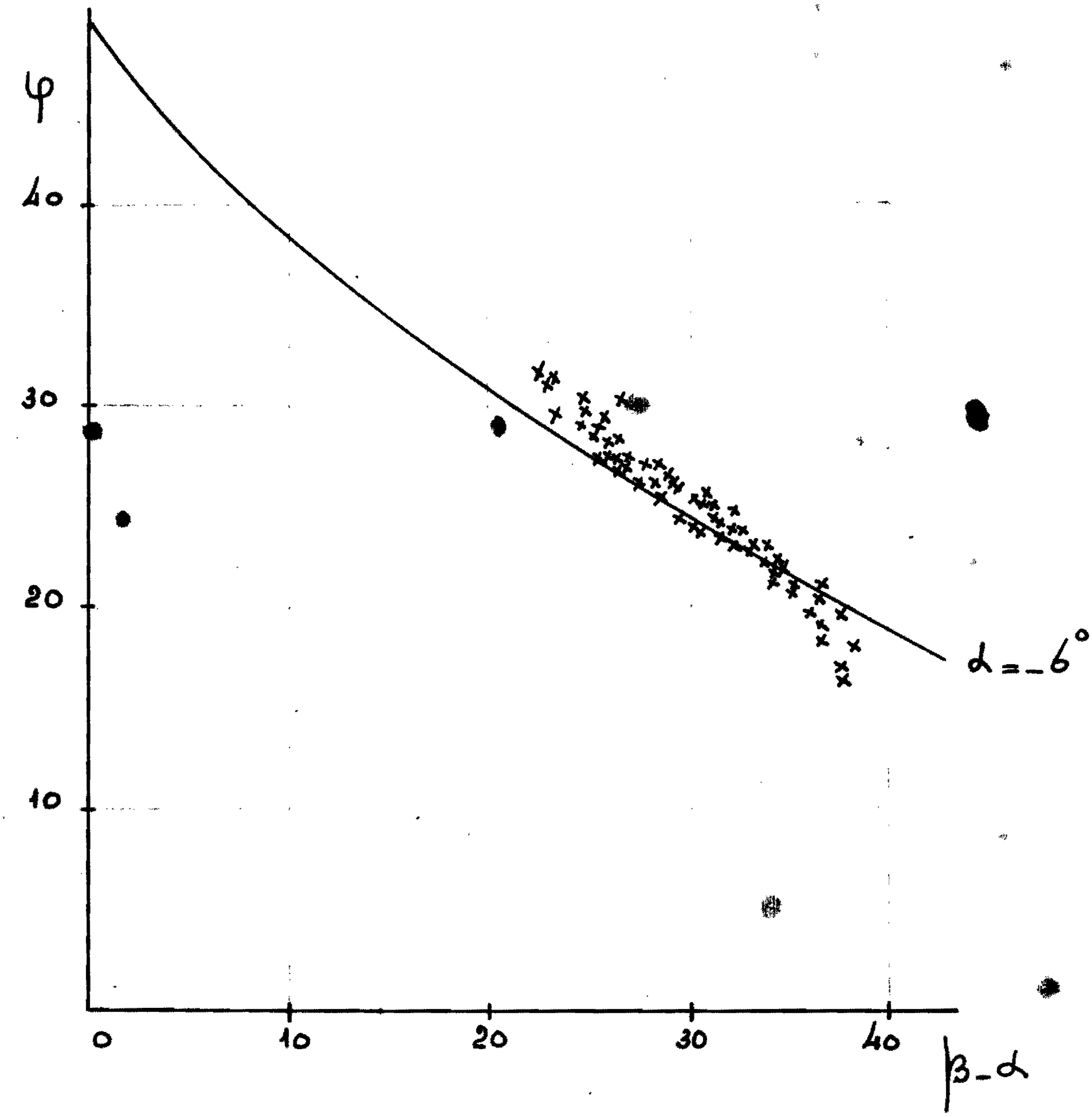

Fig. 10

The stress-strain relation of an annealed steel C 45 in metal cutting, according to eqs. 13 and 26 and based on the measurements of fig. 8.

TECHNISCHE HOGESCHOOL EINDHOVEN

LABORATORIUM VOOR MECHANISCHE TECHNOLOGIE
EN WERKPLAATSTECHNIEK

fig.10

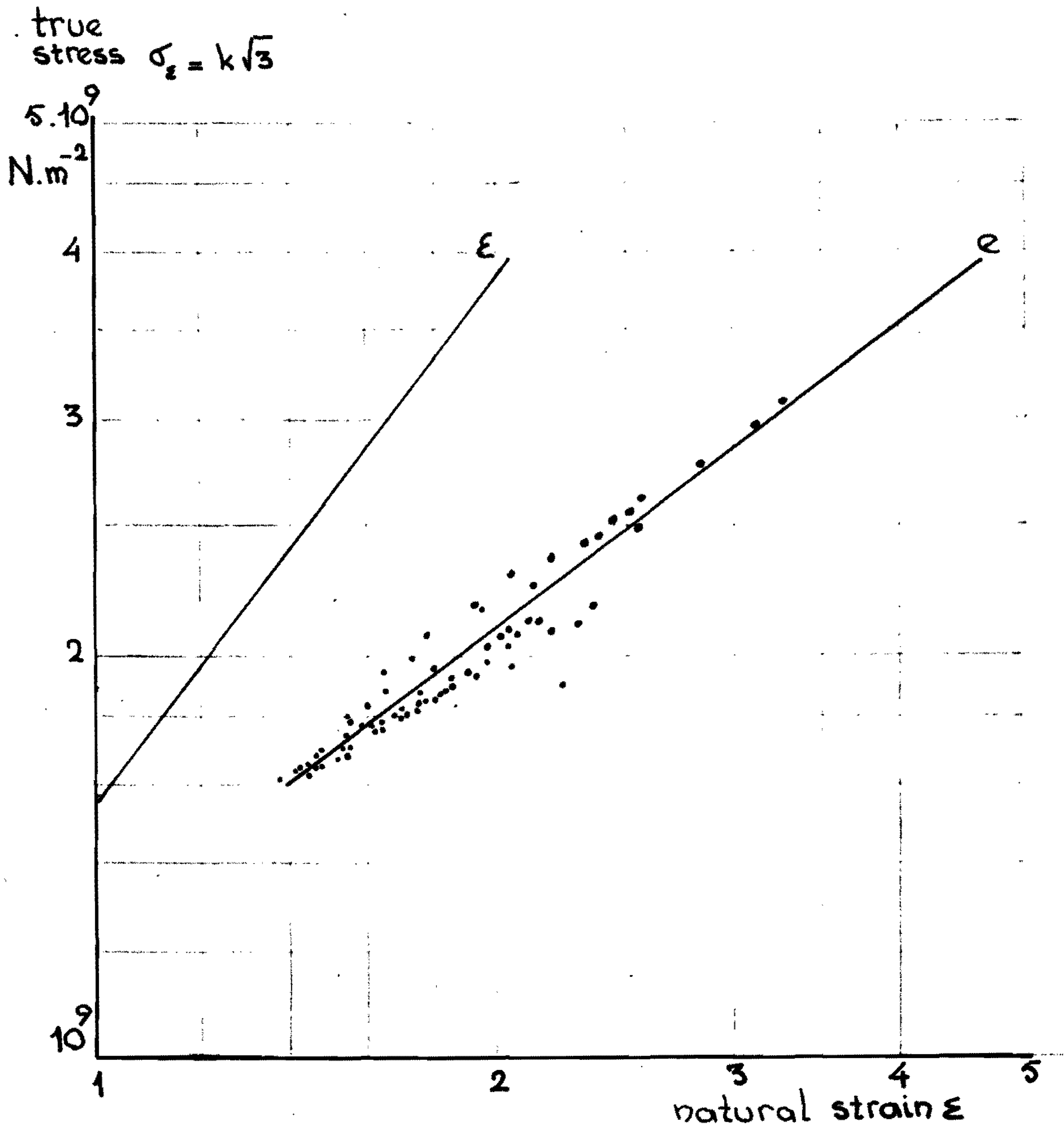

<u>Fig. 11</u>

The stress-strain relation of an annealed steel C 45 as obtained from a step by step interrupted tensile test. Yield point 3.42 10^{8} Nm^{-2} (34.2 kgf/mm^2), fracture 10^9 Nm^{-2}(100 kgf/mm^2).

TECHNISCHE HOGESCHOOL EINDHOVEN

LABORATORIUM VOOR MECHANISCHE TECHNOLOGIE
EN WERKPLAATSTECHNIEK

fig. 11

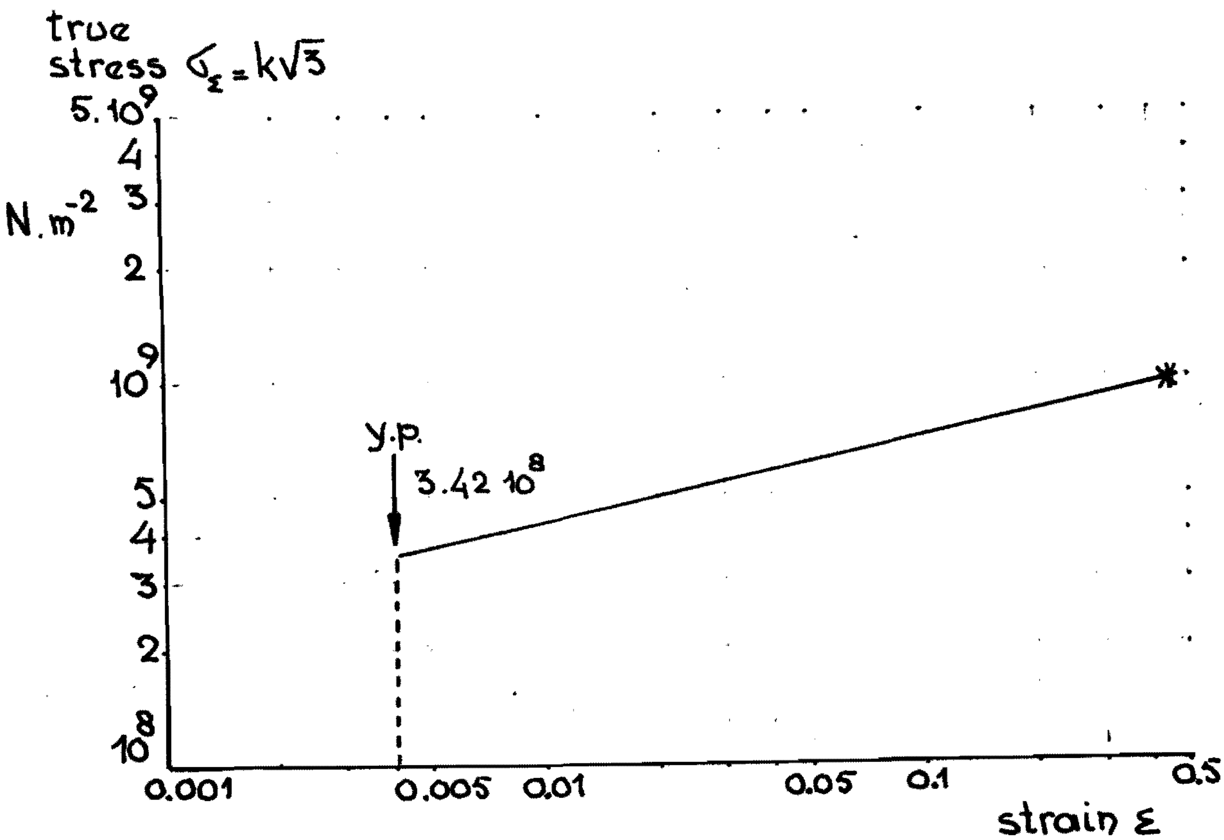

Fig. 12

Comparison of strain hardening in a tensile test and in the process of metal cutting.

TECHNISCHE HOGESCHOOL EINDHOVEN

LABORATORIUM VOOR MECHANISCHE TECHNOLOGIE
EN WERKPLAATSTECHNIEK

fig. 12

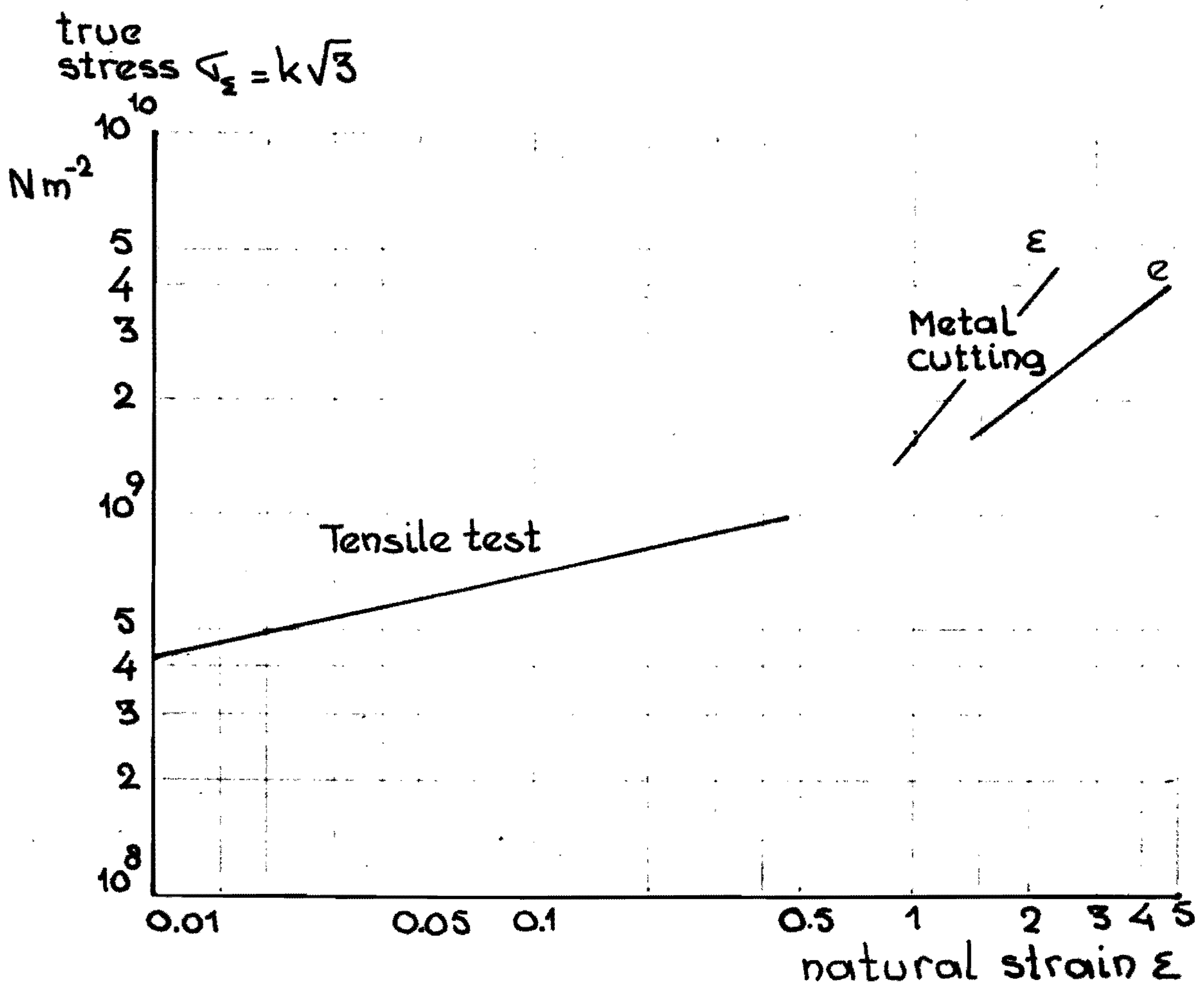

Appendix

concerning numerical values obtained by dynamometry when machining steel C 45 (annealed) with a carbide tool grade S 2(P20)

In these reports the following symbols are used:

v = cutting speed

a = feed

P_v = main cutting force

P_A = force in direction of feed, thrust force

τ_s = average shear stress in shear plane

λ = inverse value of chip thickness ratio

γ = shear strain

φ = shear angle

β = friction angle

α = rake angle

ε = true strain

μ = coefficient of friction

σ_ε = true tensile stress

The rake angle is defined in a plane passing through the direction of the cutting speed vector and the direction of the normal to the plane machined.

Table A_1	rake angle	+ 6°
	clearance angle	5°
	side cutting edge angle	15°
	nose radius	1,2 mm
	depth of cut	3 mm
Table A_2	results of calculations refering to observations A_1	
Table B_1	rake angle	+ 6°
	clearance angle	5°
	side cutting edge angle	0°
	nose radius	1,2 mm
	depth of cut	3 mm
Table B_2	results of calculations refering to observations B_1	

Table C_1	rake angle	- 6°
	clearance angle	17°
	side cutting edge angle	0°
	nose radius	1,2 mm
	depth of cut	3 mm
Table C_2	results of calculations refering to observations C_1	

The machine tool used is a lathe, type A.I.DR 200-special
input power 60/80 kW.
number of revs. 0 ÷ 5000, continuous control
range of feeds 0.0025 ÷ 40 mm/rev., continuous
control, max. cutting force 10^4N (1000 kgf).

The measurements have been performed by the metal cutting research team under the direction of Chr. Bus, ing.

Detailed information is given in the laboratory report WT 138 by A.G. Strous and H. Munnecom.

Rap-port 0139 - blz. 49

v m/sec.	0,10		0,13		0,16		0,20		0,25		0,32		0,40		0,50		0,63		0,79	
1,00	125 [1]	4,10 [2]	130	3,46	137	2,87	150	2,60	182	2,40	215	2,31	247	2,12	287	2,00	340	1,86	402	1,69
	77 [3]	83,0 [4]	80	74,3	85	71,1	90	65,5	97	68,5	104	66,0	109	64,0	110	63,0	113	63,0	115	62,5
1,12	122	4,00	127	3,30	133	2,81	155	2,55	177	2,32	210	2,17	240	2,06	282	1,92	340	1,78	407	1,69
	75	82,5	78	74,9	82	69,4	90	69,0	95	67,0	98	66,5	103	63,0	104	63,1	110	64,0	115	63,8
1,26	110	3,70	125	3,15	128	2,63	148	2,40	175	2,24	202	2,12	245	2,00	287	1,92	335	1,77	412	1,64
	70	78,0	80	74,8	78	69,4	83	68,0	88	68,5	92	64,5	100	66,2	101	65,2	102	64,0	110	64,6
1,41	113	3,70	120	2,92	132	2,56	148	2,35	172	2,20	212	2,09	237	1,95	275	1,86	335	1,75	400	1,69
	75	77,5	75	75,5	78	73,0	83	69,0	85	68,5	92	69,5	92	65,6	92	63,6	97	65,0	102	63,9
1,58	112	3,50	121	2,92	125	2,50	144	2,25	170	2,12	205	2,00	232	1,88	277	1,76	330	1,63	410	1,55
	70	82,5	73	76,8	74	69,6	78	68,5	82	69,0	86	68,0	88	64,7	89	66,1	91	65,5	100	67,3
1,78	110	3,20	115	2,69	123	2,31	140	2,05	157	2,00	190	1,87	222	1,85	277	1,77	327	1,65	398	1,54
	65	86,0	65	77,4	68	72,1	70	70,5	70	66,0	73	67,0	75	63,4	82	67,3	85	65,5	90	66,4
2,00	95	3,00	102	2,46	115	2,31	135	2,15	157	2,00	190	1,87	230	1,77	273	1,64	325	1,60	405	1,53
	58	77,0	60	70,6	63	67,8	67	67,5	70	66,0	72	67,0	79	67,1	78	67,6	82	66,0	90	67,8
2,24	90	2,50	105	2,31	120	2,13	140	2,00	163	1,92	190	1,87	230	1,73	275	1,70	330	1,59	405	1,55
	55	79,0	60	74,9	65	72,7	66	72,0	68	70,5	70	67,0	77	67,6	80	67,3	83	67,0	88	67,8
2,51	90	2,70	105	2,30	118	2,13	135	1,95	160	1,84	200	1,78	225	1,75	265	1,72	337	1,63	400	1,58
	55	77,0	60	74,9	60	73,2	63	70,5	65	70,5	73	71,5	70	67,2	73	65,8	80	69,0	85	67,3
2,82	90	2,40	105	2,16	120	2,00	140	1,85	162	1,80	192	1,72	220	1,70	277	1,66	337	1,59	400	1,58
	53	81,0	59	76,8	60	75,8	63	75,0	64	72,5	69	72,0	69	66,1	75	69,6	82	69,0	87	66,9
3,16	85	2,30	100	2,15	112	1,88	132	1,75	160	1,84	190	1,63	225	1,60	271	1,60	325	1,60	400	1,57
	51	78,0	55	73,8	57	71,0	59	71,0	65	70,5	68	69,5	68	69,0	71	69,1	75	67,0	85	67,4
3,55	83	2,40	99	2,08	115	1,94	135	1,80	155	1,65	194	1,59	225	1,53	263	1,48	323	1,50		
	47	76,0	52	75,2	54	75,0	55	74,5	55	73,0	67	72,0	65	70,0	69	67,3	75	67,0		
3,98	85	2,20	100	2,08	117	1,87	140	1,80	160	1,60	194	1,59	220	1,53	267	1,58	330	1,48		
	50	79,0	53	75,4	55	76,0	57	77,5	60	74,0	65	72,5	67	67,6	72	67,4	78	69,0		
4,47	83	2,00	95	1,85	112	1,81	130	1,70	155	1,72	192	1,57	230	1,60	275	1,54			P_v [1]	λ [2]
	48	79,5	49	74,1	50	75,3	53	73,0	55	72,5	68	71,0	71	70,4	77	69,0			P_A [3]	Z_s [4]
5,01	85	2,10	100	2,00	122	1,94	140	1,95	157	1,84	190	1,75	240	1,68					A_1	
	51	79,5	52	76,7	57	80,1	64	74,0	64	69,5	66	69,5	76	72,1						

v (m/sec) \ α	0,10		0,13		0,16		0,20		0,25		0,32		0,40		0,50		0,63		0,79	
1,00	4,14	0,77	3,54	0,77	3,02	0,78	2,78	0,75	2,61	0,68	2,54	0,62	2,39	0,57	2,30	0,51	2,19	0,45	2,08	0,40
	3,40	310	2,80	266	2,31	229	2,10	212	1,96	197	1,89	190	1,75	183	1,68	175	1,58	169	1,49	165
	14°10'	31°40'	16°30'	31°40'	19°50'	31°50'	21°50'	31°00'	23°30'	28°05'	24°20'	25°50'	26°20'	23°50'	27°50'	21°00'	29°30'	18°20'	32°10'	16°00'
1,12	4,05	0,77	3,40	0,77	2,96	0,77	2,74	0,73	2,55	0,68	2,43	0,60	2,34	0,56	2,24	0,49	2,14	0,44	2,08	0,40
	3,30	310	2,67	255	2,27	225	2,07	208	1,90	194	1,80	184	1,71	180	1,63	175	1,54	169	1,49	165
	14°20'	31°40'	17°20'	31°35'	20°15'	31°40'	22°10'	30°10'	24°10'	28°15'	25°50'	25°00'	27°00'	23°20'	28°50'	20°20'	30°45'	18°00'	32°10'	15°45'
1,26	3,77	0,80	3,27	0,80	2,81	0,76	2,62	0,71	2,59	0,64	2,39	0,59	2,30	0,53	2,24	0,47	2,13	0,42	2,05	0,40
	3,03	290	2,55	250	2,13	217	1,96	202	1,93	197	1,78	184	1,68	177	1,63	175	1,53	166	1,46	162
	15°30'	32°30'	18°10'	32°40'	21°30'	31°25'	23°30'	29°20'	25°10'	26°40'	26°20'	24°30'	27°40'	22°10'	28°50'	19°25'	30°55'	17°00'	33°00'	16°00'
1,41	3,77	0,91	3,06	0,78	2,75	0,74	2,58	0,71	2,45	0,63	2,36	0,57	2,26	0,51	2,20	0,46	2,12	0,41	2,08	0,37
	3,03	290	2,36	237	2,07	213	1,92	202	1,81	191	1,73	182	1,64	177	1,59	173	1,52	166	1,49	165
	15°30'	36°10'	19°30'	32°00'	22°05'	30°35'	24°00'	29°20'	25°30'	26°20'	26°40'	23°30'	28°20'	21°10'	29°40'	18°30'	31°10'	16°10'	32°10'	14°20'
1,58	3,58	0,78	3,06	0,76	2,70	0,74	2,49	0,69	2,39	0,62	2,30	0,55	2,21	0,51	2,13	0,44	2,04	0,39	2,00	0,36
	2,83	278	2,36	237	2,03	213	1,84	195	1,76	188	1,68	179	1,60	175	1,53	168	1,45	164	1,42	160
	16°20'	32°00'	19°30'	31°10'	22°40'	30°40'	25°00'	28°30'	26°20'	25°45'	27°40'	22°50'	29°20'	20°50'	31°00'	17°50'	33°10'	15°30'	34°40'	13°40'
1,78	3,31	0,74	2,86	0,71	2,54	0,70	2,33	0,64	2,30	0,58	2,20	0,51	2,19	0,46	2,13	0,41	2,06	0,38	1,99	0,34
	2,60	262	2,18	228	1,90	203	1,71	189	1,68	182	1,59	176	1,58	172	1,53	168	1,47	164	1,41	160
	17°50'	30°40'	21°05'	19°30'	24°20'	29°00'	27°10'	26°30'	27°45'	24°00'	29°20'	21°00'	29°45'	18°40'	30°50'	16°30'	32°50'	14°40'	34°45'	12°50'
2,00	3,13	0,77	2,67	0,74	2,54	0,69	2,41	0,63	2,30	0,58	2,20	0,51	2,13	0,47	2,05	0,40	2,02	0,37	1,98	0,33
	2,43	252	2,00	217	1,90	203	1,77	192	1,68	182	1,59	176	1,53	172	1,46	165	1,43	164	1,40	160
	19°00'	31°30'	23°00'	30°30'	24°20'	28°40'	26°10'	26°20'	27°45'	24°00'	29°20'	20°50'	30°55'	19°00'	33°00'	16°00'	33°40'	14°10'	35°00'	12°30'
2,24	2,71	0,77	2,54	0,72	2,40	0,69	2,30	0,61	2,24	0,55	2,20	0,48	2,11	0,47	2,09	0,41	2,02	0,37	2,00	0,33
	2,05	231	1,90	210	1,76	197	1,68	186	1,62	182	1,59	176	1,51	170	1,50	168	1,43	164	1,42	160
	23°05'	31°30'	24°20'	29°45'	26°10'	28°30'	27°45'	25°15'	28°50'	22°40'	29°20'	20°20'	34°30'	19°00'	34°00'	16°15'	33°50'	14°10'	34°40'	12°20'
2,51	2,87	0,77	2,54	0,72	2,40	0,65	2,26	0,60	2,18	0,53	2,14	0,49	2,12	0,43	2,10	0,39	2,00	0,35	2,01	0,32
	2,18	239	1,90	210	1,76	197	1,65	186	1,58	180	1,54	173	1,52	170	1,50	168	1,42	162	1,43	160
	21°00'	31°30'	24°30'	29°45'	26°10'	27°00'	28°20'	25°00'	29°55'	22°10'	30°40'	20°05'	31°10'	17°20'	31°40'	15°20'	33°10'	13°20'	34°00'	12°00'
2,82	2,62	0,74	2,42	0,71	2,30	0,64	2,18	0,58	2,15	0,52	2,10	0,48	2,09	0,43	2,06	0,39	2,02	0,36	2,01	0,33
	1,96	223	1,79	203	1,68	191	1,58	184	1,55	177	1,50	171	1,50	170	1,46	165	1,43	164	1,43	160
	24°05'	30°40'	25°50'	29°20'	27°45'	26°35'	29°45'	24°15'	30°30'	21°35'	31°40'	19°50'	32°00'	17°25'	32°40'	15°10'	33°50'	13°40'	34°00'	12°20'
3,16	2,53	0,75	2,41	0,70	2,21	0,65	2,12	0,58	2,18	0,53	2,04	0,48	2,02	0,42	2,02	0,38	2,03	0,34	2,01	0,32
	1,88	220	1,79	203	1,60	188	1,52	178	1,58	180	1,45	169	1,43	167	1,43	165	1,44	164	1,43	160
	24°25'	31°00'	26°00'	28°50'	29°20'	27°00'	31°10'	24°10'	29°55'	22°10'	33°10'	19°40'	33°40'	16°50'	33°40'	14°20'	35°40'	13°00'	34°10'	12°00'
3,55	2,62	0,72	2,36	0,67	2,25	0,60	2,15	0,53	2,05	0,48	2,02	0,46	1,98	0,41	1,95	0,38	1,97	0,35		
	1,96	223	1,74	200	1,68	191	1,55	181	1,46	172	1,44	169	1,40	165	1,37	161	1,39	162		
	24°05'	29°35'	26°50'	27°40'	28°30'	25°10'	30°30'	22°10'	33°00'	19°30'	33°50'	19°00'	35°00'	16°10'	36°00'	14°40'	35°30'	13°10'		
3,98	2,45	0,74	2,36	0,67	2,21	0,60	2,15	0,53	2,02	0,50	2,02	0,46	1,98	0,42	2,01	0,39	1,96	0,35		
	1,81	216	1,74	200	1,60	188	1,55	181	1,43	172	1,44	169	1,40	165	1,43	163	1,38	162		
	25°30'	30°40'	26°50'	28°00'	29°30'	25°10'	30°30'	22°10'	33°40'	20°30'	33°50'	18°30'	35°00'	17°00'	34°00'	15°10'	35°55'	13°20'		
4,47	2,30	0,73	2,19	0,66	2,16	0,58	2,09	0,53	2,10	0,48	2,01	0,48	2,02	0,43	1,99	0,40			tan γ	μ
	1,68	206	1,58	194	1,56	185	1,50	178	1,50	174	1,43	166	1,43	167	1,40	163			ε	σε
	27°40'	30°00'	29°45'	27°20'	30°20'	24°00'	32°00'	22°10'	31°40'	19°30'	34°10'	19°30'	33°40'	17°10'	34°50'	15°40'			φ	β-s
5,01	2,37	0,75	2,30	0,66	2,25	0,59	2,26	0,59	2,18	0,53	2,12	0,47	2,08	0,44						
	1,74	210	1,68	197	1,68	191	1,65	186	1,58	180	1,52	171	1,49	170					A_2	
	26°30'	31°00'	27°45'	27°30'	28°30'	24°40'	28°20'	24°35'	29°55'	22°10'	31°10'	19°10'	32°20'	17°40'						

Rapport 0139 - blz. 46

v m/sec	0,10		0,13		0,16		0,20		0,25		0,32		0,40		0,50		0,63		0,79	
1,00	110[1]	3,80[2]	117	3,16	135	2,82	153	2,65	180	2,48	214	2,25	248	2,10	295	1,98	350	1,84	420	1,71
	68[3]	77,0[4]	75	69,9	83	70,7	90	66,7	95	66,7	101	66,5	103	65,7	108	65,7	110	65,5	115	65,8
1,12	110	3,80	120	3,08	135	2,88	153	2,60	180	2,40	214	2,22	245	2,08	288	1,92	343	1,79	412	1,71
	70	76,4	75	73,4	84	68,8	89	67,4	95	67,6	99	67,1	100	65,1	100	65,5	102	69,4	105	65,7
1,26	108	3,50	111	2,85	131	2,75	150	2,55	173	2,28	205	2,16	241	2,05	283	1,86	340	1,76	405	1,65
	71	78,6	74	68,7	79	69,7	85	67,4	87	67,3	90	66,2	93	65,5	94	65,8	98	65,7	100	65,5
1,41	115	3,80	115	3,00	130	2,69	150	2,45	177	2,24	203	2,09	270	2,35	280	1,88	333	1,75	398	1,62
	71	80,2	71	71,7	75	70,4	82	69,3	88	69,3	85	67,3	125	66,3	90	65,4	90	65,2	94	64,3
1,58	113	3,40	115	2,70	132	2,50	150	2,30	180	2,12	205	2,00	242	1,95	285	1,76	337	1,71	420	1,65
	75	83,6	73	74,8	80	72,9	83	70,6	90	71,7	89	67,9	90	67,5	92	67,6	94	65,9	107	67,2
1,78	123	4,00	134	3,16	130	2,50	155	2,40	177	2,08	203	1,94	247	1,87	280	1,74	335	1,59	410	1,63
	80	82,5	80	81,7	76	72,7	85	71,8	88	71,0	85	68,8	101	67,9	90	66,7	94	66,7	103	66,0
2,00	111	3,80	127	2,93	125	2,50	146	2,30	175	2,00	203	2,03	250	1,82	280	1,72	335	1,57	407	1,62
	74	76,5	78	80,2	72	70,3	78	69,7	83	71,9	83	68,1	99	69,2	88	67,2	91	67,5	100	66,1
2,24	100	3,10	124	2,62	123	2,31	145	2,25	170	1,96	200	1,94	250	1,80	280	1,70	330	1,54	407	1,62
	59	80,3	76	82,5	69	69,2	75	70,1	78	71,1	79	68,7	97	70,2	85	68,0	90	66,3	100	66,1
2,51	95	3,00	115	2,38	122	2,31	145	2,25	167	1,88	202	2,00	250	1,77	278	1,68	350	1,63	412	1,58
	60	76,4	71	79,0	67	68,8	72	71,0	77	70,8	75	69,5	95	70,9	84	67,5	95	69,8	95	68,2
2,82	90	2,90	106	2,08	120	2,31	145	2,20	168	1,88	199	1,97	250	1,75	277	1,68	345	1,59	415	1,58
	56	73,9	65	75,4	66	67,5	70	72,8	76	71,5	75	68,7	94	71,2	81	68,3	95	69,0	96	68,6
3,16	91	2,90	106	1,93	120	2,12	145	2,25	168	1,84	197	1,91	238	1,80	285	1,66	348	1,59		
	55	75,5	60	79,0	67	71,5	71	72,2	73	72,8	73	68,6	83	68,8	85	69,8	95	69,4		
3,55	90	2,50	105	2,08	120	2,19	137	1,95	167	1,84	192	1,78	238	1,75	282	1,66	348	1,62		
	53	80,0	62	76,1	66	71,5	57	74,6	73	73,3	59	71,7	81	69,7	85	68,6	93	69,7		
3,98	90	2,30	106	2,08	119	2,06	135	1,90	167	1,88	190	1,91	240	1,75	285	1,68				
	52	83,4	60	78,3	65	73,0	57	73,3	72	72,1	60	70,2	83	69,9	85	69,8				
4,47	92	2,50	105	2,16	120	2,06	135	1,90	165	1,84	189	1,91	225	1,75					P_v [1]	λ [2]
	53	81,6	59	77,0	65	73,5	57	73,3	72	71,6	63	68,6	70	67,6					P_A [3]	τ_s [4]
5,01	92	2,50	105	2,08	115	2,06	135	1,95	170	1,84	195	1,87	225	1,75					B1	
	55	80,7	58	78,1	60	70,5	58	73,5	81	71,3	68	64,5	72	67,3						

a (mm) / v (m/sec)	0,10		0,13		0,16		0,20		0,25		0,32		0,40		0,50		0,63		0,79	
1,00	3,86[1] 3,11[3] 1510[5]	0,78[2] 2,95[4] 3150[6]	3,27 2,56 1810	0,80 2,50 3240	2,97 2,30 2010	0,77 2,09 3140	2,82 2,16 2120	0,74 2,12 3030	2,68 2,03 2250	0,67 2,01 2750	2,49 1,85 2500	0,61 1,90 2520	2,37 1,74 2630	0,54 1,83 2230	2,28 1,66 2800	0,49 1,75 2010	2,18 1,56 2950	0,43 1,71 1730	2,09 1,48 3150	0,39 1,65 1520
1,12	3,86 3,11 1510	0,80 2,95 3230	3,20 2,50 1830	0,78 2,45 320	3,03 2,35 1950	0,78 2,14 3150	2,78 2,12 2150	0,73 2,12 3010	2,62 1,97 2330	0,67 1,97 2750	2,47 1,83 2520	0,60 1,87 2450	2,36 1,73 2650	0,54 1,80 2210	2,24 1,62 2850	0,47 1,75 1910	2,15 1,54 3030	0,41 1,68 1630	2,09 1,48 3150	0,37 1,65 1420
1,26	3,58 2,85 1620	0,82 2,77 3330	3,00 2,32 2000	0,83 2,36 3340	2,91 2,24 2040	0,76 1,89 3100	2,74 2,08 2210	0,71 2,09 2930	2,52 1,88 2440	0,64 1,94 2640	2,42 1,79 2550	0,57 1,85 2340	2,34 1,71 2710	0,51 1,80 2110	2,19 1,59 2930	0,46 1,72 1830	2,13 1,52 3100	0,41 1,68 1610	2,06 1,46 3250	0,36 1,63 1350
1,41	3,86 3,11 1510	0,77 2,95 3140	3,13 2,44 1900	0,77 2,41 3140	2,86 2,19 2110	0,73 2,06 3000	2,66 2,01 2300	0,69 2,06 2840	2,48 1,84 2500	0,64 1,92 2630	2,37 1,74 2640	0,55 1,85 2240	2,57 1,93 2400	0,60 1,92 2450	2,21 1,60 2920	0,44 1,72 1750	2,12 1,50 3110	0,39 1,66 1510	2,04 1,44 3320	0,35 1,63 1320
1,58	3,49 2,77 1650	0,83 2,77 3340	2,87 2,20 2100	0,79 2,37 3220	2,70 2,04 2240	0,76 1,96 3110	2,53 1,97 2420	0,70 1,99 2900	2,39 1,76 2620	0,64 1,88 2640	2,30 1,68 2750	0,57 1,80 2330	2,26 1,64 2820	0,50 1,77 2020	2,13 1,52 3100	0,45 1,70 1800	2,09 1,48 3150	0,40 1,66 1540	2,06 1,46 3250	0,37 1,63 1420
1,78	4,05 3,28 1420	0,81 3,09 3300	3,27 2,56 1805	0,75 2,50 3050	2,70 2,04 2240	0,73 1,96 3020	2,61 1,89 2330	0,69 2,06 2850	2,36 1,73 2650	0,63 1,85 2630	2,25 1,63 2830	0,55 1,80 2250	2,20 1,59 2920	0,54 1,75 2220	2,11 1,50 3120	0,44 1,67 1750	2,02 1,42 3350	0,40 1,63 1540	2,04 1,44 3310	0,37 1,63 1410
2,00	3,86 3,11 1505	0,83 2,95 3340	3,86 2,38 1930	0,83 2,41 3135	2,70 2,04 2270	0,72 1,96 2950	2,53 1,89 2420	0,68 1,99 2810	2,30 1,68 2750	0,60 1,84 2530	2,32 1,70 2720	0,54 1,82 2220	2,17 1,56 3010	0,52 1,71 2140	2,10 1,49 3140	0,44 1,67 1730	2,00 1,40 3410	0,39 1,61 1510	2,04 1,44 3320	0,36 1,63 1350
2,24	3,22 2,52 1825	0,74 2,56 3030	2,80 2,14 2140	0,77 2,24 3130	2,53 1,89 2430	0,71 1,89 2920	2,49 1,85 2500	0,66 1,99 2730	2,28 1,66 2820	0,59 1,84 2440	2,25 1,63 2830	0,52 1,80 2130	2,16 1,55 3030	0,51 1,71 2110	2,09 1,48 3200	0,42 1,67 1700	1,99 1,38 3450	0,39 1,61 1520	2,04 1,44 3320	0,36 1,63 1350
2,51	3,13 2,44 1900	0,79 2,51 3220	2,60 1,95 2340	0,77 2,17 3140	2,53 1,89 2430	0,70 1,89 2850	2,44 1,85 2500	0,62 1,99 2540	2,20 1,59 2940	0,58 1,80 2440	2,30 1,68 2750	0,49 1,80 2020	2,14 1,53 3050	0,51 1,71 2050	2,07 1,46 3210	0,42 1,67 1700	2,04 1,44 3310	0,39 1,63 1510	2,01 1,40 3400	0,34 1,60 1300
2,82	3,04 2,35 1940	0,78 2,43 3155	2,36 1,73 2650	0,77 2,00 3135	2,53 1,89 2430	0,70 1,89 2850	2,44 1,80 2500	0,62 1,95 2540	2,20 1,59 2940	0,58 1,80 2410	2,28 1,66 2810	0,50 1,80 2040	2,12 1,51 3110	0,50 1,69 2040	2,07 1,46 3210	0,41 1,67 1620	2,02 1,42 3350	0,39 1,63 1520	2,01 1,40 34°	0,34 1,60 13°
3,16	3,04 2,35 1940	0,76 2,43 3110	2,25 1,63 2840	0,71 1,97 2930	2,37 1,74 2630	0,71 1,83 2920	2,49 1,85 2500	0,63 1,99 2610	2,18 1,56 2950	0,56 1,78 2520	2,23 1,61 2850	0,49 1,76 2020	2,16 1,55 3030	0,47 1,71 1920	2,06 1,45 3240	0,42 1,65 1640	2,02 1,42 3350	0,39 1,63 1520		
3,55	2,71 2,05 2305	0,74 2,30 3030	2,36 1,73 2650	0,74 2,00 3030	2,45 1,81 2530	0,70 1,87 2850	2,26 1,64 2810	0,54 1,87 2220	2,18 1,56 2950	0,57 1,78 2530	2,14 1,53 3050	0,43 1,74 1710	2,12 1,51 3110	0,46 1,69 1850	2,06 1,45 3240	0,42 1,65 1700	2,03 1,43 3320	0,38 1,63 1500		
3,98	2,53 1,88 2425	0,73 2,19 3000	2,36 1,73 2650	0,71 2,00 2930	2,34 1,71 2700	0,70 1,80 2840	2,22 1,60 2900	0,55 1,83 2250	2,21 1,60 2920	0,56 1,80 2320	2,23 1,61 2850	0,44 1,80 1730	2,12 1,51 3110	0,47 1,69 1920	2,07 1,46 3210	0,42 1,67 1640				
4,47	2,71 2,05 2305	0,72 2,30 2955	2,42 1,78 2550	0,71 2,10 2920	2,34 1,71 2700	0,68 1,80 2820	2,22 1,60 2900	0,55 1,83 2250	2,18 1,56 2950	0,56 1,78 2320	2,23 1,61 2850	0,45 1,80 1830	2,12 1,51 3110	0,43 1,69 1720					tan γ [1] ε [3] ψ [5]	u [2] σε [4] β·s [6]
5,01	2,71 2,05 2305	0,75 2,30 3050	2,36 1,73 2650	0,70 2,00 2900	2,34 1,71 2700	0,66 1,80 2730	2,26 1,64 2820	0,56 1,87 2320	2,18 1,56 2920	0,60 1,78 2530	2,20 1,58 2930	0,47 1,76 1920	2,12 1,51 3110	0,44 1,69 1740					B 2	

v (m/sec) \ mm	0,10		0,13		0,16		0,20		0,25		0,32		0,40		0,50		0,63		0,79	
1,00	135	4,40	152	3,54	158	3,32	170	2,80	206	2,60	239	2,38	277	2,15	332	2,02	410	1,84	—	—
	110	77,9	118	78,3	120	69,0	125	65,4	138	67,5	150	64,5	159	64,0	178	64,0	202	66,0	—	—
1,12	132	4,20	140	3,39	150	3,15	165	2,70	195	2,48	233	2,28	272	2,08	328	1,88	409	1,76	—	—
	105	78,4	110	73,5	115	66,8	119	64,3	131	65,0	145	64,0	154	64,0	172	65,0	198	66,6	—	—
1,26	125	3,90	130	3,23	143	2,94	164	2,55	191	2,36	228	2,19	269	2,03	325	1,86	405	1,73	—	—
	98	79,0	104	69,8	105	67,2	115	66,2	126	65,0	138	64,5	147	64,0	165	65,0	190	66,8	—	—
1,41	115	3,60	123	3,00	137	2,75	162	2,45	190	2,28	224	2,09	266	1,95	326	1,80	400	1,62	—	—
	90	76,1	96	69,0	102	66,3	112	67,0	122	65,5	132	64,5	142	64,6	159	66,5	210	64,0	—	—
1,58	106	3,30	120	2,84	135	2,56	161	2,35	187	2,20	220	2,03	263	1,85	315	1,74	400	1,58	—	—
	84	73,3	95	68,6	98	67,0	105	68,8	117	66,5	126	64,5	137	65,5	150	65,3	209	65,5	—	—
1,78	101	3,10	118	2,69	132	2,50	154	2,25	182	2,12	218	1,97	261	1,77	305	1,68	392	1,55	—	—
	79	72,0	90	69,7	92	67,4	100	67,0	104	67,8	120	65,5	128	66,5	145	63,7	204	63,0	—	—
2,00	116	3,30	115	2,62	135	2,44	155	2,20	179	2,08	215	1,94	257	1,75	305	1,66	392	1,53	—	—
	88	81,5	82	70,5	90	70,5	99	71,0	102	66,9	113	65,6	125	66,0	141	64,5	203	63,0	—	—
2,24	106	3,10	115	2,54	130	2,31	154	2,15	175	2,04	210	1,91	255	1,75	309	1,66	380	1,54	—	—
	81	77,0	81	71,8	88	69,0	95	70,0	99	65,8	109	64,8	122	66,0	140	65,6	160	66,5	—	—
2,51	105	2,90	110	2,46	129	2,25	153	2,10	174	1,96	210	1,87	254	1,70	310	1,64	380	1,56	—	—
	79	79,0	76	70,0	85	70,0	92	70,0	96	66,8	106	65,8	120	66,5	139	66,5	162	66,0	—	—
2,82	92	2,70	108	2,31	127	2,19	150	2,05	173	1,92	210	1,84	253	1,70	306	1,62	390	1,57	—	—
	67	72,0	73	70,6	81	70,0	89	69,5	94	66,8	105	66,2	119	66,5	137	65,6	165	67,5		
3,16	90	2,70	106	2,23	126	2,13	147	2,00	174	1,88	210	1,84	253	1,65	296	1,64	—	—		
	64	71,0	70	70,6	80	70,0	87	69,0	94	67,8	103	66,6	116	67,5	126	64,2	—	—		
3,55	89	2,60	106	2,15	125	2,06	149	1,95	172	1,88	209	1,84	256	1,65	310	1,66				
	62	71,5	69	71,8	78	70,5	86	70,5	88	68,1	99	67,5	118	68,0	131	67,4				
3,98	89	2,60	106	2,15	124	2,06	143	1,95	170	1,84	210	1,82	260	1,68	—	—				
	60	73,0	68	72,1	77	70,0	76	69,5	87	67,6	103	67,0	120	68,5	—	—				
4,47	89	2,50	108	2,33	125	2,06	142	1,85	170	1,84	215	1,78	—	—					P_v (1)	λ (2)
	61	73,0	69	72,0	78	70,5	76	70,0	88	67,5	106	68,5	—	—					P_A (3)	Z_s (4)
5,01	86	2,50	110	2,33	126	2,06	150	2,00	—	—	—	—							C 1	
	59	71,0	71	73,0	78	71,0	90	69,0	—	—	—	—								

v (m/sec.) \ α (mm)	0,10		0,13		0,16		0,20		0,25		0,32		0,40		0,50		0,63		0,79	
1,00	4,83 [1]	1,01 [2]	4,03	0,96	3,83	0,94	3,37	0,91	3,19	0,83	3,01	0,79	2,83	0,72	2,72	0,68	2,59	0,63	—	—
	4,08 [3]	346 [4]	3,27	280	3,08	262	2,64	233	2,48	220	2,30	208	2,15	196	2,05	190	1,93	183	—	—
	12°30' [5]	39°20' [6]	15°20'	37°50'	16°20'	37°10'	19°	36°10'	20°20'	33°50'	22°	32°10'	24°	29°50'	25°10'	28°10'	27°15'	26°15'	—	—
1,12	4,64	0,99	3,89	0,97	3,68	0,95	3,28	0,89	3,09	0,84	2,93	0,78	2,77	0,71	2,61	0,67	2,54	0,62	—	—
	3,88	324	3,13	272	2,94	254	2,56	228	2,39	215	2,24	204	2,09	195	1,96	185	1,89	181	—	—
	13°05'	38°40'	16°	38°10'	17°10'	37°40'	19°40'	35°40'	21°10'	34°	22°50'	31°50'	24°40'	29°30'	26°50'	27°40'	28°15'	25°50'	—	—
1,26	4,36	0,97	3,75	0,99	3,49	0,91	3,15	0,87	2,99	0,82	2,86	0,76	2,73	0,69	2,61	0,65	2,52	0,60	—	—
	3,60	308	3,00	265	2,76	244	2,45	221	2,30	210	2,17	200	2,06	193	1,95	185	1,87	180	—	—
	14°	38°	16°40'	38°40'	18°40'	36°10'	20°40'	35°	22°10'	33°30'	23°30'	31°10'	25°10'	28°40'	27°	27°	28°40'	25°10'	—	—
1,41	4,09	0,97	3,54	0,96	3,32	0,92	3,07	0,86	2,85	0,80	2,78	0,74	2,67	0,68	2,57	0,63	2,45	0,67	—	—
	3,35	294	2,80	252	2,60	235	2,36	217	2,17	204	2,10	197	2,01	190	1,92	183	1,81	177	—	—
	15°10'	38°	17°50'	38°	19°20'	36°30'	21°25'	34°40'	23°05'	32°40'	24°30'	30°30'	26°	28°10'	27°45'	26°	30°10'	27°40'	—	—
1,58	3,71	0,98	3,40	0,98	3,16	0,91	2,99	0,81	2,87	0,78	2,73	0,72	2,60	0,66	2,53	0,61	2,43	0,66	—	—
	2,96	272	2,67	246	2,44	226	2,29	214	2,18	204	2,05	194	1,94	187	1,88	182	1,79	176	—	—
	16°20'	38°20'	18°50'	38°20'	20°40'	36°10'	22°10'	33°	23°30'	32°	25°10'	29°50'	27°10'	27°30'	28°30'	25°30'	30°50'	27°30'	—	—
1,78	3,63	0,97	3,27	0,94	3,11	0,87	2,90	0,81	2,80	0,71	2,69	0,70	2,55	0,63	2,49	0,61	2,40	0,66	—	—
	2,88	267	2,55	238	2,40	224	2,21	208	2,12	201	2,02	192	1,90	184	1,85	180	1,76	175	—	—
	17°20'	38°	19°40'	37°20'	21°	35°	23°	33°	24°10'	29°20'	25°50'	28°50'	28°10'	26°10'	29°20'	25°30'	31°30'	27°30'	—	—
2,00	3,81	0,94	3,21	0,88	3,06	0,83	2,87	0,73	2,77	0,72	2,67	0,67	2,53	0,62	2,48	0,60	2,40	0,66	—	—
	3,06	283	2,50	236	2,35	221	2,18	212	2,10	200	2,00	191	1,88	184	1,83	179	1,76	175	—	—
	16°20'	37°10'	20°10'	35°30'	21°30'	33°50'	23°30'	30°10'	24°35'	29°40'	26°10'	27°45'	28°20'	25°50'	29°40'	24°50'	31°30'	27°30'	—	—
2,24	3,63	0,94	3,14	0,87	2,95	0,84	2,83	0,76	2,74	0,72	2,65	0,66	2,53	0,62	2,48	0,59	2,40	0,55	—	—
	2,88	267	2,42	231	2,26	216	2,15	206	2,06	198	1,98	190	1,88	184	1,83	179	1,76	175	—	—
	17°20'	37°10'	20°40'	35°10'	22°30'	34°10'	24°	31°10'	25°	29°30'	26°30'	27°10'	28°20'	25°40'	29°40'	24°30'	31°20'	22°50'	—	—
2,51	3,45	0,93	3,08	0,86	2,90	0,82	2,79	0,75	2,68	0,70	2,62	0,65	2,50	0,61	2,46	0,58	2,41	0,55	—	—
	2,71	258	2,38	229	2,21	214	2,11	203	2,02	195	1,96	189	1,85	182	1,82	178	1,77	176	—	—
	18°20'	36°50'	21°20'	34°40'	23°	33°30'	24°30'	31°	25°50'	28°50'	26°50'	26°50'	29°	25°30'	29°50'	24°10'	31°	23°	—	—
2,82	3,28	0,91	2,95	0,84	2,86	0,80	2,75	0,74	2,65	0,69	2,60	0,64	2,50	0,60	2,45	0,58	2,42	0,55	—	—
	2,56	247	2,25	222	2,18	210	2,07	201	1,99	193	1,94	188	1,85	182	1,81	178	1,78	176	—	—
	19°40'	36°10'	22°30'	34°	23°30'	32°40'	25°	30°30'	26°20'	28°30'	27°15'	26°40'	29°	25°10'	30°10'	24°10'	30°50'	23°	—	—
3,16	3,28	0,92	2,89	0,82	2,81	0,79	2,71	0,74	2,63	0,68	2,60	0,63	2,47	0,59	2,46	0,56	—	—		
	2,56	247	2,20	218	2,13	209	2,04	200	1,97	193	1,94	188	1,83	181	1,82	178	—	—		
	19°40'	35°20'	23°10'	33°30'	24°10'	32°30'	25°30'	30°30'	26°50'	28°20'	27°15'	26°10'	29°40'	24°40'	29°50'	23°10'	—	—		
3,55	3,19	0,87	2,83	0,81	2,76	0,77	2,67	0,71	2,63	0,66	2,60	0,61	2,47	0,59	2,48	0,55				
	2,48	242	2,16	215	2,08	206	2,00	198	1,97	193	1,94	188	1,83	181	1,83	179				
	20°20'	35°	24°	33°	24°50'	31°50'	26°	29°50'	26°50'	27°10'	27°15'	25°30'	29°40'	24°40'	29°40'	23°				
3,98	3,19	0,83	2,83	0,80	2,76	0,77	2,67	0,67	2,60	0,66	2,58	0,63	2,49	0,59	—	—				
	2,48	242	2,16	215	2,08	206	2,00	198	1,94	191	1,92	187	1,85	182	—	—				
	20°20'	33°50'	24°	32°40'	24°50'	31°50'	26°	28°	27°20'	27°10'	27°40'	26°10'	29°20'	24°40'	—	—				
4,47	3,11	0,85	2,97	0,80	2,76	0,77	2,60	0,68	2,60	0,66	2,55	0,63	—	—					tang α [1]	μ [2]
	2,41	238	2,27	223	2,08	206	1,94	194	1,94	191	1,90	186	—	—					ε [3]	σ_z [4]
	21°	34°20'	22°20'	32°35'	24°50'	31°50'	27°10'	28°10'	27°20'	27°20'	28°	26°20'	—	—					φ [5]	β-3 [6]
5,01	3,11	0,86	2,97	0,81	2,76	0,77	2,76	0,75	—	—	—	—							C 2	
	2,41	238	2,27	223	2,08	206	2,08	201	—	—	—	—								
	21°	34°40'	22°20'	32°50'	24°50'	31°50'	25°30'	31°	—	—	—	—								